Chemistry–A European Journal
Review
doi.org/10.1002/chem.202101572

Check for updates

Chemistry Europe
European Chemical Societies Publishing

Polymer Nanodiscs and Their Bioanalytical Potential

Michelle D. Farrelly,[a] Lisandra L. Martin,*[a] and San H. Thang*[a]

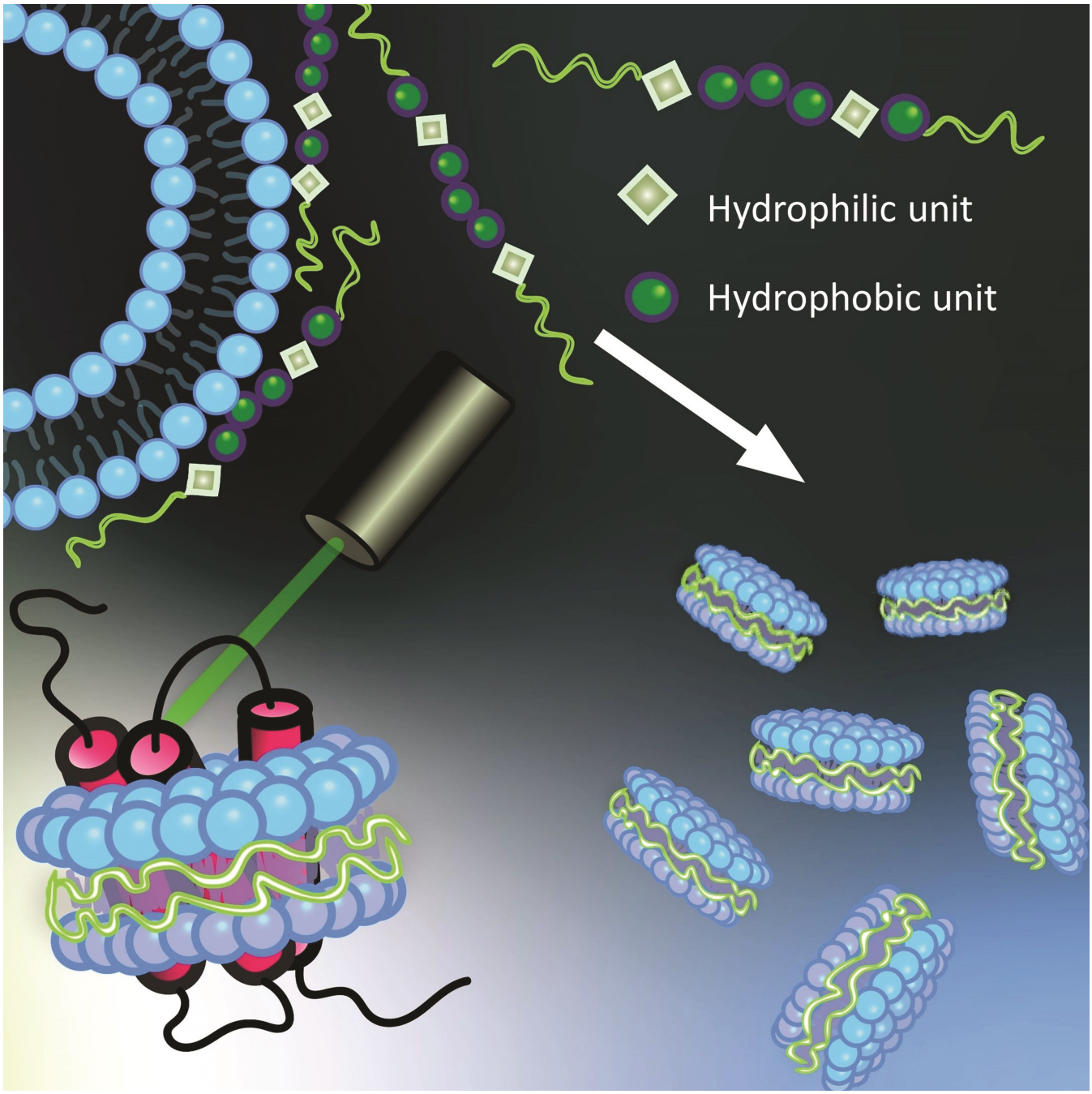

© 2021 Wiley-VCH GmbH

Abstract: Membrane proteins (MPs) play a pivotal role in cellular function and are therefore predominant pharmaceutical targets. Although detailed understanding of MP structure and mechanistic activity is invaluable for rational drug design, challenges are associated with the purification and study of MPs. This review delves into the historical developments that became the prelude to currently available membrane mimetic technologies before shining a spotlight on polymer nanodiscs. These are soluble nanosized particles capable of encompassing MPs embedded in a phospholipid ring. The expanding range of reported amphipathic polymer nanodisc materials is presented and discussed in terms of their tolerance to different solution conditions and their nanodisc properties. Finally, the analytical scope of polymer nanodiscs is considered in both the demonstration of basic nanodisc parameters as well as in the elucidation of structures, lipid–protein interactions, and the functional mechanisms of reconstituted membrane proteins. The final emphasis is given to the unique benefits and applications demonstrated for native nanodiscs accessed through a detergent free process.

1. Introduction

Membrane proteins (MPs) are critical to the regulatory functions of cells, instrumental in intercellular signalling, selective transport, cellular structure and metabolism.[1,2] Peripheral membrane proteins, largely hydrophilic and associated with either the inner or outer surface of the phospholipid bilayer, as well as integral membrane proteins which contain a hydrophobic transmembrane domain penetrating through the cell membrane in between intra- and extra-cellular domains, are both MP classes functionally reliant on their specific lipid environment. Although MPs have significant cellular consequence rendering them predominant targets for pharmaceutical products, they are underrepresented in the protein database due to the inherent difficulties involved in their purification and biophysical characterisation which also retains their structural integrity.[3–4]

1.1. Membrane mimetic technology: A brief history

Among the first established methodologies of studying membrane proteins in a lipid bilayer simulating environment included the reconstitution of MPs into synthetic lipid monolayer films, supported lipid bilayers (SLBs), tethered bilayer lipid membranes and liposomes mediated by the initial solubilisation of MPs by detergent micelles (Figure 1).[2,3,5] Lipid monolayer films consist of a 2D planar sheet of lipids in a single leaflet extended across an amphipathic interface, being either the solid–water (such as upon SiO_2) or the air–water interface. Such monolayer surfaces are useful for surface pressure isotherms of embedded MPs and techniques apt to probe the protein orientation and surface coverage of reconstituted proteins, such as X-ray and neutron reflectivity.[2,6] Limitations of monolayers not simulating the double leaflet bilayer property of membranes explains the heightened relative popularity of SLBs, which are extended planar lipid bilayers often generated by Langmuir–Blodgett transfer or liposome (lipid vesicle) fusion onto a SiO_2 or modified gold surface.[7] SLBs are undoubtedly suitable for reconstituting certain peripheral and integral membrane proteins (which protrude through one membrane side) for use in surface sensitive measurement approaches including quartz crystal microbalance with dissipation monitoring[8] and total internal reflection fluorescence[6,9] of protein association properties. However, integral membrane proteins take up space on both intra- and extracellular sides of the lipid bilayer sheet to varying degrees, a property which is often better accommodated by tethered lipid bilayers making use of macromolecules such as polymer cushions. Tethering materials act as spacers that link the lipid bilayer either non-covalently (as with polymer cushions) or covalently to the solid support whilst reducing compressive stress between bilayer incorporated MPs and the analytical surface.[3,7] Advances in

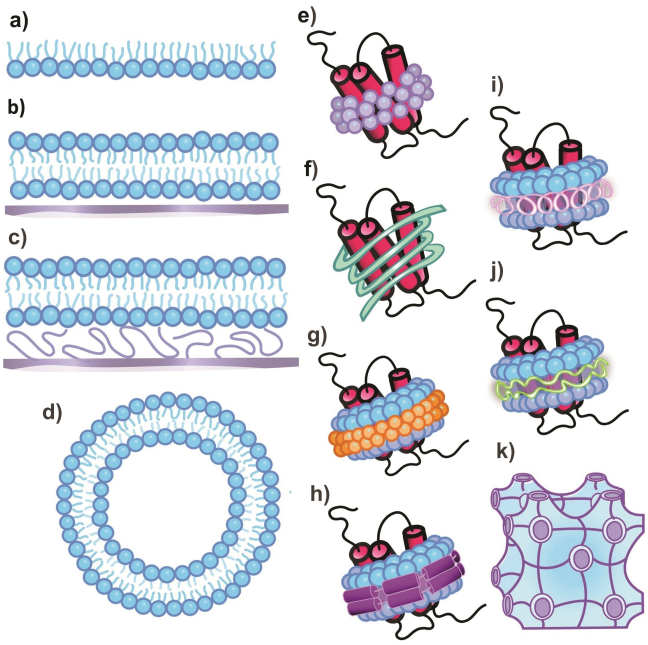

Figure 1. Illustrations of membrane mimetics that can be applied to the characterisation and study of membrane proteins. a) lipid monolayer film, b) supported lipid bilayer, c) tethered lipid bilayer, d) liposome, e) detergent micelle, f) amphipol, g) bicelle, h) membrane scaffold protein (MSP) nanodisc, i) peptidisc, j) polymer nanodisc and k) lipid cubic phase.

[a] *M. D. Farrelly, Prof. L. L. Martin, Prof. S. H. Thang*
School of Chemistry, Monash University
Clayton, 3800, Vic (Australia)
E-mail: Lisa.Martin@monash.edu
San.Thang@monash.edu

© 2021 Wiley-VCH GmbH

polymer cushion materials, such as amphipathic maleic acid based polymers, have the added advantage of being able to swell to an extent related to their alkyl functionality chain length, providing a space of up to 45–60 nm between a solid SiO_2 surface and lipid bilayer without impeding lateral mobility of MPs. Bilayers have also been directly tethered by covalent linkage to lipids or proteins.[10]

Liposomes are spherical vesicles composed of lipid bilayer which can reconstitute MPs to become proteoliposomes. As a membrane mimetic, liposomes offer the unique advantage of a distinguished enclosed inner membrane region within the vesicle and an outer membrane space allowing for the monitoring of protein function by measuring the intake or expulsion of compounds such as ions between aqueous compartments for transporter protein channels.[2,3,5] Solid state NMR and the patch-clamp method are among techniques applicable to understanding protein structure and activity within proteoliposomes.[11,12] In some instances, the curvature of liposomes (related to their lipid composition) can induce stress to which some protein's activities are sensitive. Moreover, it is a challenge to concentrate proteins in liposomes which limits their signal in biophysical measurements.[2]

Against this pre-existing membrane mimetic landscape which involved embedding multiple MPs into an extended surface, emerged the introduction of compact nanosized particles able to encompass individual proteins or protein complexes with greater stability than detergent micelles which have a propensity toward aggregation and denaturation of proteins.[13–14] One of these nanoparticle systems are amphipols, a class of amphipathic polymeric surfactant with an acrylamide backbone developed by Popot and co-workers.[4,15] Amphipols directly coil around the hydrophobic transmembrane domain of MPs which are first stabilised in aqueous solution by detergent.[16] The compact monodisperse size and enhanced stability of amphipols particles makes them appropriate candidates for cryo-EM and native mass spectroscopy investigations of constituent MPs.[17] The direct interaction between the hydrophobic moieties of the amphipol polymer and the MP do mean that amphipols can still, however, disrupt the structure of sensitive proteins.[14]

Bicelles were another nanoscale cassette introduced to reconstitute individual MPs, in this case into solubilised membrane bilayer disks.[18] Particles consist of discoidal long-chain phospholipid lipid bilayers encircled by a rim of short-chain lipid or detergent. The ability to tune the size of bicelles by varying the molar ratio, the q value, of the long-chain to short-chain lipid component (often as $q = [DMPC]/[DHPC]$; DMPC: 1,2-dimyristoyl-*sn*-glycero-3-phosphocholine, DHPC: 1,2-dihexanoyl-*sn*-glycero-3-phosphocholine), led to the preparation of small isotropic ($q < 1.5$) and large magnetically alignable ($q > 2.5$) bicelles amenable to solution and solid-state NMR studies of MPs respectively.[11,19] For example, solid state NMR was used to probe the structure and mobility of 72 kDa cytochrome b5 (cyt b5) and cytochrome P450 (cyt P450) complex in magnetically aligned bicelles.[20] Past constraints on the applicable temperature range for solid-state NMR studies with bicelles, which is influenced by the phase-transition temperature of phospholipids and enables detrimental heating effects, has been addressed by the introduction of temperature resistant bicelles comprised of long-chain 1,2-didecanoyl-*sn*-glycero-3-phosphocholine (DDPC) and short-chain 1,2-diheptanoyl-*sn*-glycero-3-phosphocholin (DHepPC) lipids, showing an active temperature range of −15 to 80 °C and an enhanced spectral sensitivity to MP structure.[21] An amenability towards X-ray crystallography applications has also been demonstrated for bicelles wherein MP crystals can be reliably grown in the membrane mimicking phospholipid bilayer disc.[22] Bicelles possess their own limitations in their requirement for specific

Michelle Farrelly is a current PhD candidate at Monash University in the field of polymer chemistry with specific interest in the biochemical applications of RAFT polymers. Michelle completed a BSc and BA double degree from Monash University (Melbourne, Australia) in 2018 with majors in chemistry and philosophy. The following year, she completed her honours in chemistry where she began her research into novel polymer nanodiscs.

Lisa Martin is an Associate Professor in Chemistry at Monash University. She received her BSc from Monash University and her PhD from The Australian National University. After three years' postdoctoral experience in Switzerland, Germany (Alexander von Humboldt Fellowship) and the USA (Fulbright Fellowship), she began her academic career at Flinders University, then moved to Monash University in 2003. Her research is at the interface of chemical biology and medicinal chemistry, and she has pioneered methods for studying membrane proteins and peptides at biomimetic membrane interfaces. She is a Fellow of the Royal Society of Chemistry (UK) and the Royal Australian Chemical Institute.

San Thang completed his PhD in chemistry at Griffith University in 1987. Following a research career at CSIRO (1986-2014), he is now a Professor of Chemistry at Monash University. His research focuses on the interface between biology and polymer chemistry. He has an h-index of 56. He is responsible for several key inventions in the area of controlled/living radical polymerisation, significantly, as a co-inventor of the RAFT process. He is a Fellow of the Australian Academy of Science, of the Australian Academy of Technology and Engineering, and of the Royal Australian Chemical Institute. In 2018, he was made a Companion of the Order of Australia.

© 2021 Wiley-VCH GmbH

types of lipid in a strict ratio for their formulation and the possibility for the short chained lipid or detergent species to diffuse into the lipid bilayer and denature the protein encapsulated.[23]

In the early 2000s, Sligar and co-workers[24] reported the discovery and compelling applications of membrane scaffold protein (MSP) nanodiscs. These are comprised of a non-covalent arrangement of phospholipid and two genetically engineered amphipathic α-helical MSPs, based on human serum apolipoprotein A-I.[3] High density lipoprotein (HDL) is involved in cholesterol transport in the human body with apolipoprotein A-I as its primary protein constituent. After its initial synthesis in the liver, HDL progresses through an transient intermediate discoidal bilayer structure before becoming a spherical particle ready to carry out its transport function.[25] It was the ability to synthetically harness the intermediate MSP nanodisc assembly by either mixing detergent with excess lipid, MSP and the starting cellular membrane or adding MSP and lipid to the pre-micellised MP in an optimised stoichiometry, followed by rapid removal of detergent which gave rise to stabile, size-controlled and monodisperse nanodiscs.[24–25] Similarly to bicelles, the MPs within nanodiscs were stabilised within a lipid bilayer environment with the competitive advantage of enhanced stability of MSP nanodiscs over time compared to bicelles.[26] The monodispersity conferred from the ability to adjust the diameter of nanodiscs between 7 and 20 nm by choosing an engineered MSP variant of a certain length, gave this membrane mimetic system the power to selectively capture particular sized proteins or oligomeric forms of integral membrane protein assemblies.[27–28] Furthermore, large nanodiscs ranging from 70–90 nm have been recently achieved utilising a DNA origami scaffold to recruit and merge small MSP nanodiscs with excess lipid into DNA corralled nanodiscs.[29,30] Analytical platforms are available for membrane proteins solubilised by MSP nanodiscs where stability and uniformity of structure are important such as electron microscopy (EM)[31] and small-angle X-ray scattering (SAXS).[25] Single-molecule fluorescence (SMF) measurements can be attained in which nanodiscs are anchored to a surface with MSP or lipid-labelled affinity tags so as not to disturb the subtle conformational changes in MPs monitored by single particle fluorescence intensity measurement. For surface tethered nanodiscs, proteins are solvent and ligand accessible from both intra- and extracellular sides of the membrane, a notable point of distinction compared to SLBs or tethered lipid bilayers which can be studied and accessed only from the solvent exposed and visible surface.

As MSP nanodiscs became the favoured MP reconstitution method, more synthetic or bio-engineered amphipathic peptides were developed and used as nanoscale membrane mimetics. These included engineered nanostructured β-sheet peptides[32] as well as "peptidiscs" which are a term that encompasses monohelical synthetic 18 amino acid peptides (2F and 4F), bihelical nanodisc scaffold peptide (NSP)[33] and reversed sequence amphipathic bi-helical peptide (NSPr).[34] Nanostructured β-sheet peptides directly stabilise reconstituted MPs within a barrel structure held together by hydrogen bonding between β-strands upon a detergent dialysis procedure. The ATP-binding-cassette (ABC) exporter protein MsbA (bacterial homologue) retained higher functional activity after β-sheet peptide reconstitution compared with the exporter in detergent micelles and produced electron micrographs of the solubilised protein with a low detergent background. Peptidiscs have more in common with MSP nanodiscs as they also solubilise MPs surrounded by a ring of lipid bilayer. Forms of the peptidisc have been able to directly solubilise lipids into empty nanodiscs from liposomes, although, peptidiscs have not yet been shown to solubilise MPs directly from their native membrane without detergent mediating the reconstitution. Size modulation of peptide nanodiscs is achieved by changing the phospholipid/peptide ratios whereas for MSP nanodiscs, the appropriately sized scaffold protein must be used in a strict optimised lipid/MSP/MP ratio for a successful MP reconstitution to occur.[33–34] The 4F peptidisc has been employed for the first demonstration of the fusion of nanodiscs and the collision mediated spontaneous exchange of lipids between nanodiscs in real time high speed atomic force microscopy along with ^{31}P NMR analysis.[35] 4F has also been used for ^{19}F NMR studies of the lipid and cyt P450 protein interaction with ^{19}F-labelled microsomal cyt b5 protein.[36] SapA, a saposin protein-based lipid nanoparticle (SapNP) is similarly amphipathic and able to encircle MPs entrapping a minimal number of stabilising annular lipids. These nanoparticles are tuneable in size depending on the lipid/saposin component ratio and were shown to be able to reconstitute functional MPs containing 14 to 56 transmembrane helices.[37] The convenience in capturing MPs in peptidisc variants and SapNPs is expected to lead to an increased future adoption of these membrane mimetics.

Lipid cubic phase (LCP) has become an increasingly adopted medium for characterising integral membrane proteins, such as G protein-coupled receptors (GPCRs), by X-ray crystallography.[3,25] The LCP assembly is a bicontinuous (extending in two directions) sheet of lipid bilayer which forms a 3D mesophase exhibiting cubic symmetry formed from a particular monoacylglycerol lipid-water mixture.[38] Within this sticky and viscous cubic phase, an MP can (in the presence of precipitants) be reconstituted and crystallised yet at the same time can theoretically diffuse freely within the 3D sheet. Although the mobility of MPs can present a problem for X-ray crystallography using LCP media, high resolution crystal structures of MPs, particularly for those with small soluble domains, have been generated, examples include diacylglycerol kinase and an engineered human β 2-adrenergic GPCR.[39–40] The number of steps required to be reoptimised for each new MP partitioned into LCP are inconveniently high as different detergents and conditions are often required for the solubilisation, stabilisation and crystallisation of MPs into this membrane mimetic system. Ways to refine this technique to make it more easily accessible and less time consuming are being pursued.[25]

Detergent micelles, typically non-ionic detergents such as Triton X-100, *n*-dodecyl-β-D-maltoside (DDM), employed at some stage for each of the MP reconstitution techniques discussed so far, are in a way their own membrane mimetic system which have long been the conventional method for the purification of discrete membrane proteins and form a cassette

© 2021 Wiley-VCH GmbH

for their analysis in aqueous solutions.[11,41] Interference with the folding of proteins by direct interaction between detergent molecules and the transmembrane protein domain as well as the removal of annular lipids surrounding the MP critical to protein structure and stability, are the major drawbacks in using detergents as membrane mimetics or mediators in the reconstitution process of proteins.[23,42] Selecting the correct detergent to dissolve a selected protein proves to be an arduous process largely achieved by trial and error. Alternative agents which can directly dissolve MPs and which also escape the shortcomings of detergent micelles were keenly welcomed in the field of protein biophysics.[14] The range of membrane mimetics surveyed in this paper are summarised in Figure 1.

2. Polymer Nanodiscs

2.1. Styrene maleic acid lipid particles (SMALPs)

Answering the call for MP reconstituting membrane simulants which do not necessitate the use of mediating detergent, is a copolymer of styrene and maleic anhydride subsequently hydrolysed into amphipathic polystyrene-co-maleic acid (SMA). This amphipathic copolymer, with its structure and synthetic route shown in Scheme 1, was the first of a collection of synthetic polymers which form second-generation nanodiscs.

Nanodiscs resulting from SMA are referred to as styrene maleic acid lipid particles. SMALPs are formed by directly extracting membrane proteins either from native cellular membranes (giving native nanodiscs) or from an intermediary MP-reconstituted synthetic membrane system to ultimately form self-assembled nanodisc structures of a general 10–12 nm diameter.[4] Post extraction, MPs retain their surrounding ring of phospholipid bilayer as the SMA coils around the discoidal membrane bundle through the hydrophobic styrene groups being thermodynamically driven to intercalate into the lipid tail groups as carboxylate groups of the maleic acid orient toward the outside of the nanodisc allowing for its dissolution in aqueous media.[4,43] SMALPs show no selectivity towards lipid type which gives SMA a general applicability to a wide range of integral MPs.[44] The mechanism by which SMALPs have been documented to form entails the charged partially deprotonated carboxylate groups of SMA binding to the charged hydrophilic surface of the membrane.[4] A low molar ratio of polymer/lipid is required for the membrane surface to reach a phase boundary

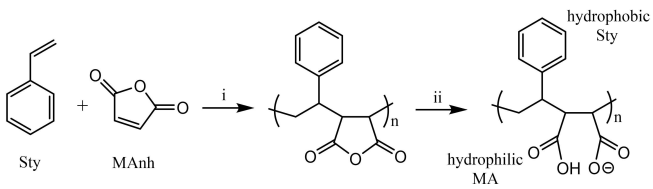

Scheme 1. The generalised synthetic route to prepare SMA copolymers. The steps include i) polymerisation of styrene and maleic anhydride and then ii) hydrolysis (promoted by base) converting maleic anhydride (MAnh) units to maleic acid (MA).

of saturation (R^{SAT}), after which polymers insert into the hydrophobic core of the membrane, forming intermediate structures and packaging membrane bundles into nanodiscs. As more SMA is introduced, the phase boundary of complete nanodisc solubilisation is reached (R^{SOL}) and all lipid has been solubilised by polymer.[43,45] The demonstration of SMALPs as a monodisperse MP reconstitution system was initially reported by the groups of Dafforn and Overduin[46] in 2009, although the interaction of SMA with phospholipids to generate disc shaped structures (now known as empty lipid nanodiscs), was previously established and investigated for use as a drug delivery system years preceding this discovery.[47]

Size tuning of SMA based copolymer nanodiscs occurs in a similar manner to the size tuning of peptide nanodiscs, the diameter can be increased by using lower polymer/lipid stoichiometric ratios and furthermore, the adjustment of styrene (Sty) and MA monomer ratios has been found to result in distinct nanodisc sizes of 28 + 1 nm for a 2:1 ratio, 10 + 1 nm for a 3:1 Sty/MA ratio and 32 + 1 nm for a 4:1 Sty/MA monomer ratio for an overall weight ratio of 1.25:1 SMA to lipid.[48] Molecular weights of SMA copolymers, on the other hand, often have a negligible effect on nanodisc size with lower molecular weight polymers offering improved size control.[14,48] A general polymer weight range of 1.5–30 kDa has accepted effectiveness in SMALP formation.[49]

At a physiological pH of 7–8, Sty/MA monomer ratios of 2:1 and 3:1 are most commonly used due to their optimal efficiency for nanodisc extraction from phospholipid bilayers.[43] Abilities of SMA to create monodisperse nanodiscs with size flexibility facilitates the reconstitution of a range of oligomeric MPs and MP complexes for analysis by various studies including fluorescence microscopy, NMR[48] and single-particle cryo-EM.[50] Beyond not inviting the destabilising effects of detergent micelles into the MP reconstitution process for native SMALP nanodiscs, an advantage of SMA and other synthetic polymer nanodiscs is that the polymers have distinct spectral properties from encapsulated MPs, whereas MSP, peptide and protein based nanodisc agents exhibit similar chemical bonds and functional groups to that of the solubilised MP which may hinder membrane protein spectroscopic analysis.[23]

Opportunities to modulate polymer sequence, chain length and monomer composition can also allow for the selection of certain desired properties of these second-generation nanodiscs. When using reversible addition fragmentation chain transfer (RAFT) polymerisation methods for instance, the SMA sequence produced is naturally alternating between Sty and MA units until styrene, which is in excess during the batch polymerisation, forms a terminating hydrophobic tail block.[43] Whereas in a statistical version of SMA, like the commercial Malvern polymer Lipodisq®, monomers are evenly distributed throughout the polymer chain sequence in proportion to their ratio as well as exhibiting greater dispersity (Đ) in chain length.[51,52] The alternating SMA (altSMA) accessed by RAFT has demonstrated a more negative free-energy change associated with the vesicle to nanodisc transition than the statistical version (coSMA). Additionally, altSMA saturates and inserts into lipid bilayers at a lower polymer/lipid ratio although complete

© 2021 Wiley-VCH GmbH

nanodisc solubilisation occurs at a similar polymer/lipid ratio. This sequence dependence of SMA insertion behaviour illustrates the influence of the hydrophobic effect on the initial propensity for the polystyrene tail block of altSMA to insert into the hydrophobic core of phospholipid bilayers.[43] For RAFT SMA polymers, conjugation of the RAFT end-group terminating each SMA copolymer so there is single moiety of interest (such as a fluorophore) on each polymer,[53] may introduce a potential site for tethering SMALPs to an analytical surface. Although no such strategy has yet been achieved for SMA. In fact, surface tethering from the stabilising polymer belt has not yet been developed for SMALPs as has been extensively demonstrated for MSP nanodiscs allowing access to both sides of the tethered bilayer. It remains questionable whether such a tethering strategy is possible due to polymer mobility and polymer exchange between nanodiscs found to occur in solution.[54]

As is true for all other membrane mimetics, there are limitations that exist for SMALPs. This includes a pH dependent ability for SMA to reconstitute MPs as carboxylic acid groups of maleic acid have consecutive pK_a values of around 6 and 10.[4] For an acidic pH range, the first deprotonation event resulting in half of all carboxylic acids becoming negatively charged carboxylates is precluded from occurring. Thus, the polymer is not hydrophilic enough to be water soluble and thereby associate with the hydrophilic membrane surface in acidic conditions.[55]

Divalent cations such as Mg^{2+} and Ca^{2+} which are often essential in the regulation and activity of transport channels and enzymes, are chelated by carboxylate groups and thus at certain concentrations lead to the precipitation of SMA.[23] Restricted tolerance to acidic pH and divalent metals constrains the scope of MPs able to be studied with SMALPs. It has recently been reported polymer nanodiscs preserve protein activity when the overall protein charge matches that of the polymer belt, meaning that SMA with a net negative charge may not be most suitable for the reconstitution of cationic proteins and hence the generality displayed by SMA towards lipid type is not fully extended towards all MPs.[56] Many of these limitations can be addressed by selecting alternative polymeric nanodisc materials which optimally perform under different conditions and analytical applications to SMALPs, the original second-generation polymer nanodiscs.

2.2. Functionally modified SMAnh derivatives: SMADs

The need to synthesise polymers able to form nanodiscs of different charges and tolerant to a range of buffer properties such as low pH and metal cation presence, has motivated the endeavour to modify SMAnh, the precursor to SMA, into a diverse range of polymers. A nucleophilic addition to the electrophilic maleic anhydride moiety of SMAnh followed by a ring opening hydrolysis step, has led to the range of polymers shown in Figure 2a) with various R groups modulating the properties of polymers.[23,57] Each of these derivatives attained by nucleophilic addition and ring opening, showed an enhanced viability under lower pH values compared to SMA

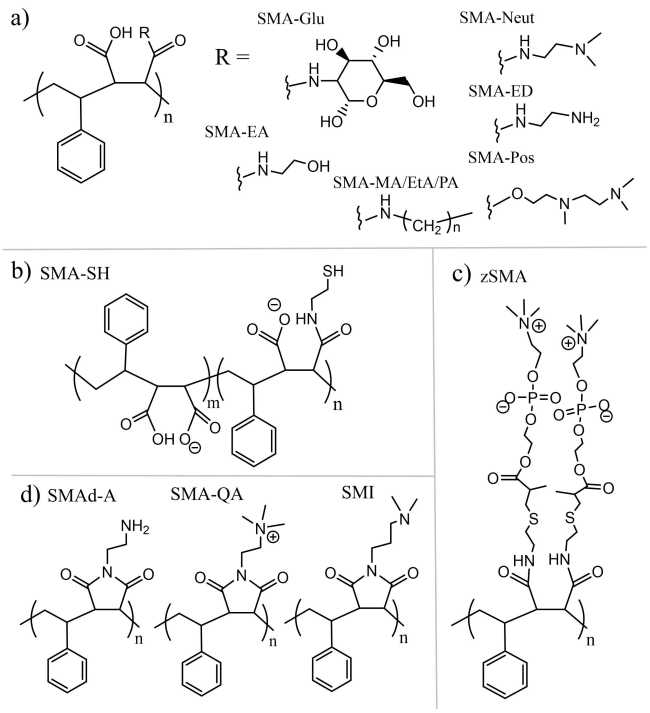

Figure 2. Summary of nanodisc-forming polymer agents synthesised from the functionalisation of SMAnh, referred to as SMADs. a) includes SMA-Glu (poly(styrene-co-maleic anhydride D-glucosamine),[57] SMA-EA (poly(styrene-co-maleic anhydride ethanol amine),[23] SMA-MA/EtA/PA (poly(styrene-co-maleic anhydride alkylamines),[61] SMA-Neut (poly(styrene-co-maleic anhydride *N*,*N*-dimethylethylenediamine),[57] SMA-ED (poly(styrene-co-maleic anhydride ethylene diamine),[23] SMA-Pos (poly(styrene-co-maleic anhydride 2-{[2-(dimethylamino)ethyl]methylamino ethanol.[55] b) represents SMA-SH (polystyrene-co-maleic acid with solvent-exposed sulfhydryls),[62] c) illustrates zSMA (zwitterionic styrene-maleic amide copolymers)[63–64] and d) which shows the styrene and maleimide copolymers SMAd–A (poly(styrene-co-maleimide–amine)),[65] SMA-QA (poly(styrene-co-maleimide–quaternary ammonium))[65] and SMI (poly(styrene-co-maleimide)).[66]

which aggregates beneath pH ~ 6.3. SMA-Glu and SMA-EA produce copolymers with a negative charge and are active nanodisc agents in pH ranges of above pH ~ 3 and ~ 3.3, respectively. Low molecular weight (1.6 kDa) SMA-EA has additionally been shown to form "macrodiscs" of up to 50 nm at low polymer to lipid ratios which align in an external magnetic field and therefore can be probed in detail by solid state NMR.[58] Recently, a SMA-EA precursor has been modified by attaching a stable metal chelator moiety, 2-aminoethyl-monoamide-DOTA, in a ratio of one DOTA group per polymer belt to form SMA-EA-DOTA, thus allowing for the stable chelation of paramagnetic metal ions such as Cu^{2+}, Gd^{3+} and Dy^{3+} which have shown effectiveness in speeding up the data acquisition times for NMR studies involving nanodiscs.[59–60] SMA-Neut was shown to be insensitive to all pH values tested, an observation explained by its continuity across the pH scale of at least a positively charged ammonium group (in more acidic environments) or a negatively charged carboxylate group (deprotonated under more basic conditions). Interestingly, SMA-ED which can also exhibit a negatively charged carboxylate and a positively charged amine, precipitates at near neutral environ-

© 2021 Wiley-VCH GmbH

ment pH ~ 6 ± 1, while being functional at the acidic and basic ends of the pH scale. The net positive polymer, SMA-Pos is highly sensitive to pH ~ 5 but tolerates pH ~ 3 and pH above ~ 6.3, which suggests the net positive charge of the polymer occurs at an acidic pH and is virtually neutral at around pH ~ 5. Each of the SMADs discussed (Figure 2a) represent a subset of possible nucleophilic additions to SMAnh and were demonstrated as more tolerant to divalent metal concentrations than SMA.

Moreover, their diversity in charge lead to their compatibility for extracting similarly charged MPs. Negatively charged human potassium voltage-gated channel subfamily E member 1 protein encoded by the KCNE1 gene (KCNE1), at neutral pH, was reconstituted into both polyanionic SMA-Glu and SMA-AE nanodiscs. SMA-Glu was shown to best retain protein dynamics by continuous wave electron paramagnetic resonance spectroscopy line-shape analysis.[57] Use of methylamine, ethylamine and propylamine R substituents (SMA-MA, SMA-EtA and SMA-PA) derived from 1 : 1 SMAnh copolymers was found to alter the size and shape of *Escherichia coli* membrane native nanodiscs. The methylamine substituted polymer assembled into monodispersed nanodiscs of smaller size (~ 14 nm), while the longer alkyl derivatives formed worm-like nanostructures which tended towards aggregation.[61] This highlighted the importance of sufficient charge density within hydrophilic SMAD copolymer units.

Zwitterionic styrene-maleic amide copolymers (zSMAs) in Figure 2c) have been similarly introduced to combat buffer incompatibilities of SMA. Such zSMAs are formed where the maleic acid groups of SMA are replaced with maleic amide moieties bearing zwitterionic phosphatidylcholine (PC) groups. Proteins reconstituted in zSMALPs, such as proton pump proteorhodopsin, can be studied in the appropriate a low pH environment due to zSMA polymers functioning across acidic and basic pH values (between pH 4 and 10).[63–64] In the presence of increasing concentrations of divalent cations, zSMAs remain effective at generating nanodiscs and their zwitterionic nature imparts them with a general compatibility with MPs of different net charges. A unique feature of zSMA which distinguishes it from all other polymer nanodisc materials reported in this paper, is the linear relationship between the molecular weight of the polymer and the diameter of resultant zSMALPs.[63] This suggests the possibility of controlling the size of zSMALPs for specifically sized protein complexes through polymer design much like the size tuning of MSP nanodiscs.

The reactivity of maleic anhydride to alcohols and amines has been exploited to partially conjugate SMAnh with cysteamine into SMAnh-SH*x* and then hydrolysed into SMA-SH*x*, being essentially SMA with solvent-exposed sulfhydryls, where *x* is the average number of sulfhydryls per SMA polymer.[62] Due to inherent heterogeneity of polymer length and sequence, even for low chain dispersities, the reaction cannot be tuned to generate singly –SH grafted polymers. This SMAnh modification was made with the intention of producing fluorescent dye and biotin labelled SMALPs through a thiol–maleimide click reaction which circumvents the need for direct membrane protein modification. FRET experiments using Alexa Fluor 488 C5 maleimide or DyLight488-labeled avidin (D488-avidin) as a reporter for binding of biotinylated SMA-SH_3, confirmed the successful labelling of SMALPs. Fluorescent Alexa Fluor 488 C5 and D488-avidin labels served as FRET donors to Atto647 N-labeled lipids within the nanodiscs. It was proposed that SMA-SH nanodiscs offer an opportunity to immobilise SMALPs to a surface with the solvent-exposed sulfhydryls docking onto gold or attaching to other surface media via these reported biotinylated SMALPs. A demonstration of this suggested surface immobilisation strategy is yet to be reported.

A ring-closing procedure upon nucleophilic addition of a hydrophilic moiety and hydrolysis of SMAnh polymers, can yield several possible poly(styrene-co-maleimide) positively charged polymer variants shown in Figure 2d) amenable to nanodisc formation. SMILPs (SMI lipid particles) compared to traditional SMA nanodiscs were shown to be smaller than SMALPs, thus placing limitations on the size of reconstituted MPs. Furthermore, SMI is less efficient at MP solubilisation from biological membranes than SMA.[6] SMAd-A and SMI are able to solubilise MPs into nanodiscs below a neutral pH of ~ 7–7.5 whilst displaying remarkable tolerance to divalent metal ions.[65–66] SMA-QA contains an ammonium group which is consistently charged independent of pH value, allowing for a broad applicability across pH and buffer conditions.[65–66]

2.3. Other nanodisc forming polymers

Each of the mentioned SMAnh derivative polymers retain styrene as their hydrophobic monomer. Because the hydrophobic effect propelling styrene insertion into membranes is the thermodynamic driving force for nanodisc assembly, many SMADs reliably demonstrate nanodisc assembly. Although the presence of styrene is not always desirable for spectroscopic studies which are styrene sensitive such as thioflavin-T (ThT) based fluorescence, UV absorption and circular dichroism (CD).[23] Laurdan is a fluorescent probe that detects changes in membrane phase properties through its sensitivity to the polarity of its environment within the bilayer.[67] It has also been found using Laurdan fluorescence that at temperatures above the phase-transition temperature (T_m) for lipid bilayers, there was no marked increase in lipid mobility within SMALPs, suggesting that many constituent lipids interact with SMA copolymer in a way which perturbs the dynamic bulk lipid properties seen in liposomes.[25,68] Given that hydrophobic styrene plays an instrumental role in membrane insertion and lipid acyl chain- polymer interactions, it is worthwhile to investigate the potential of synthetic polymers which do not contain styrene or aromatic moieties for nanodisc construction.

DIBMA (Figure 3a) is an example of an alternating copolymer similar to SMA in its inclusion of maleic acid without the spectral interference of Sty functionalities resulting from their replacement with aliphatic diisobutylene units. This polymer which demonstrates efficiency in solubilising phospholipid bilayers into (DIBMALP) nanodiscs of ~ 15 nm, can extract MPs directly from biological membranes into native nanodiscs, has a comparatively mild influence on lipid-acyl chain order and is

© 2021 Wiley-VCH GmbH

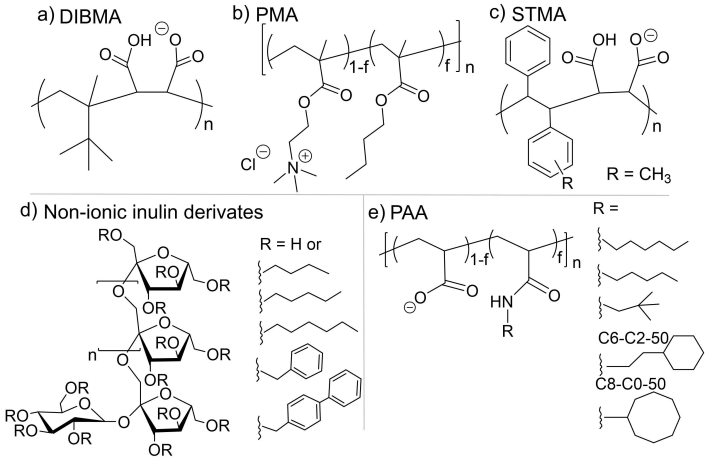

Figure 3. Nanodisc-forming polymer materials reported with alternative hydrophobic monomers to styrene: a) DIBMA (alternating poly(diisobutylene-co-maleic acid),[69] b) PMA (statistical polymethacylate with butyl methacrylate and cationic methacroylcholine chloride units),[70] c) STMA (methyl-substituted alternating poly(stilbene-co-maleic acid))[71] d) Non-ionic inulin derivatives partially substituted with butyl, pentyl, hexyl, benzyl and 4-phenylbenzyl hydrophobic groups.[72] e) PAA (hydrophobic functionalised poly(acrylic acid)) with hexyl, pentyl, neopentyl and cyclic alkanes bearing groups (C_6-C_2-50 and C_8-C_0-50).[16,73]

tolerant to low-millimolar divalent cation concentrations.[69] Far-UV CD spectra of proteins in nanodiscs could be acquired with a low extinction coefficient for DIBMA whereas CD spectra of SMALPs can be obtained only after the removal of empty nanodiscs owing to SMA spectral interference. Raman spectroscopy used to probe the conformational order of lipid bilayers, showed similar vibrational spectra before and after liposome solubilisation by DIBMA whereas SMA extraction produced significant shifts and reductions in band intensity indicative of decrease lipid acyl chain order. DIBMA has become commercially available as Sokalan CP9 (BASF, Germany) and its advantages and availability have led to its increased adoption in MP extraction.

Another class of polymer which avoids the strong light absorption of styrene is amphiphilic PMA displayed in Figure 3b).[70] A positively charged random rather than alternating sequence of hydrophilic methacroylcholine chloride and hydrophobic butyl methacrylate comprises the copolymer, facilitating its nanodisc assembly upon incubation with DMPC liposomes as well as intact (*E. coli*) cell membranes. The hydrophobic fraction (*f*) of 7–14 kg.mol^{-1} copolymers used was between 0.4–0.6 and their assembly into 17 nm discoidal nanodiscs was confirmed by cryo-electron microscopy and corroborated by differential scanning calorimetry (DSC) monitoring of bilayer T_m in conjunction with ^{31}P NMR studies. PMALPs were used to stabilise a helical intermediate in the aggregation of Human islet amyloid polypeptide associated with type 2 diabetes, which was observed with the aid of CD and (ThT) fluorescence experiments.

Sharing similarities in monomer chemical structure with SMA, methyl functionalised poly(stilbene-co-maleic acids) in Figure 3c), have been demonstrated as efficient for solubilising synthetic and native cellular membrane components into nanodiscs within the expanded pH range of 5–10.[71] More interesting advantages of STMAs, however, are conferred from their strictly alternating sequence owing to the inability for either monomer to homopolymerise as well as the increased rigidity of the polymer backbone. Precise regulation over the sequence and length of polymer chains for synthesised STMA copolymers resulted in an enhanced homogeneity of size (~20 nm) and structure of assembled nanodiscs. Initially, turbidity observations accompanied by ^{31}P NMR studies after incubation with DMPC liposomes validated the potential of STMAs to form nanodiscs and the further ability of STMAs to directly extract Lipid A palmitoyltransferase PagP monomers and dimers into native nanodiscs was revealed. Control over nanodisc homogeneity is a needed advancement for the improved structural resolution of MPs in analytical methods such as cryo-EM and native mass spectrometry.[17]

Derived from the natural polymer inulin ($M_n = 2.2$ kg mol^{-1}, DP = 14) extracted from chicory root, new non-ionic nanodisc forming polymers (Figure 3d) were developed by partial hydrophobic functionalisation with butyl, pentyl, hexyl, benzyl and 4-phenylbenzyl R groups.[72] The optimal degree of hydrophobic functionalisation (DS) was found to encompass the range 0.3–0.5 (with a maximum possible 3 DS with respect to each monomer) by turbidity monitoring and static light scattering measurement after addition of pentyl-inulin to DMPC liposomes. For each respective R group functionalised inulin polymer, a broad pH range stability of 2.5–8.5, a tolerance to 100 mM concentrations of divalent cations and the ability to directly solubilise *E. coli* membranes with a significantly higher efficiency than SMA was demonstrated. The uncharged nature of these polymers circumvents unwanted electrostatic interactions between the polymer belt and MPs granting a compatibility of functionalised inulin polymers for extracting MPs of various overall charges. ^{31}P NMR spectroscopy revealed the magnetic alignment of non-ionic polymer nanodiscs comprised of 1:1 (*w/w*) pentyl-inulin and DMPC lipid, indicating an

© 2021 Wiley-VCH GmbH

amenability of these polymers towards solid-state NMR characterisation of MPs.

Random sequence hydrophobic functionalised PAAs, hexyl-, pentyl- and neopentyl-PAA (Figure 3e), were synthesised by modifying commercial low-molecular-weight PAA and were treated with DMPC lipids to form 7–17 nm diameter nanodiscs with size dependence on polymer/lipid ratio.[73] The rationale for testing this PAA polymer as a nanodisc material, was that PAA with fractions of octyl and isopropyl side chains, is recruited for the formation of amphipols which reconstitute pre-micellised MPs, but are not effective for direct protein extraction from membranes. Inspiration from these amphipol polymers has led to the exploration of smaller alkyl groups than octyl sidechains. Using smaller pendant chains did in fact form nanodiscs after polymer addition to liposomes which, unlike styrene, were transparent to (254 nm) light absorption and had a mild effect on lipid acyl chain order validated by DSC and ^{31}P NMR. Moreover, alkylPAAs have a similar efficacy to SMA in directly extracting MPs from cellular membranes. The effect of using cyclic alkane moieties in PAA polymer membrane solubilisation, was studied with C_6-C_2-50 and C_8-C_0-50 "CyclApols" illustrated in Figure 3d. With a hydrophobic unit fraction of 0.5, comprised of eight-carbon moieties much like many amphipols, CyclApols alternatively use cycloalkanes to mimic styrene in SMA.[16] These UV-transparent CyclApols were able to directly extract YidC-GFP protein from *E. coli* membrane fragments in a higher yield than amphipols, SMA and DIBMA. Extraction efficiency of CyclApols was also shown for the native purple membrane from *Halobacterium salinarum*, a notoriously resistant membrane to polymer solubilisation after dilution with a minimal amount of DMPC lipid which was less than that required for SMA extraction. The resulting CyclApols were found to be significantly smaller than SMALPs and more research remains to be conducted into the amount of lipid copurified with MPs and whether extracted lipids retain the physical characteristics of phospholipid bilayers.

3. Nanodisc Purification and Characterisation

The successful assembly of nanodisc particles after polymer incubation with either synthetic or native membranes, is typically confirmed by more than one analytical approach. Corroborating evidence which reinforces nanodisc formation is provided by a strategy which combines several methods including, but not limited to; turbidity monitoring,[34] ^{31}P NMR,[45] electron paramagnetic resonance spectroscopy (EPR),[74] isothermal titration calorimetry (ITC),[45] surface pressure isotherms,[28] DSC,[73] Raman spectroscopy,[69] Laurdan fluorescence,[62] dynamic light scattering (DLS),[75] static light scattering, detector-coupled size-exclusion chromatography (SEC),[43] SAXS, small-angle neutron scattering (SANS),[25] analytical ultracentrifugation,[76] transmission electron microscopy (TEM),[49] microfluidic diffusional sizing (MDS)[77] and electrophoresis methods.[78] As a rule of thumb, techniques which measure the size and or shape of nanoscale discs such as DLS, SEC, MDS and SAXS are complementary to ones which give information on the polymer–lipid interaction or the nature of the lipid environment upon liposome solubilisation, that is, whether lipid bilayer ordering is retained and the distinctness of nanodisc lipids from liposome lipids. Informative methods on the nanodisc solubilised lipid environment include DSC, Raman spectroscopy and ^{31}P NMR.

Most measurements are obtained after incubating polymers with phospholipid bilayers in the form of liposome dispersions or native biological membrane fragments except for surface pressure isotherms which initially use a monolayer film at the water-air interface. A high surface pressure increase for the lipid monolayer, signals membrane insertion behaviour of the polymer, an important step in the mechanism of nanodisc assembly.[55] Stoichiometry and thermodynamic traits of polymer–lipid bilayer interactions can be attained with ITC which is sensitive to binding events.[45] Turbidity monitoring is often conducted using a spectrophotometer with optical density readings at 350 nm recorded minutes after mixing a liposome suspension with solubilising polymer. Time-dependent turbidity measurements model the kinetics of membrane extraction from turbid liposome mixtures into polymer nanodiscs which are clear in solution after complete solubilisation.[34] DSC, EPR, Raman spectroscopy and Laurdan fluorescence each provide data on lipid physical properties including conformational order, fluidity and in the instance of DSC, gel to liquid crystalline T_m. For EPR, paramagnetic centres are attached to phospholipids to allow spin probing of lipid bilayers at different depths giving information about packing and mobility of lipids at different positions in nanodiscs.[74] The intensities and band positions of Raman vibrational spectra indicate the degree of order in the lipid bilayer before and after polymer solubilisation whereas Laurdan fluorescence uses a lipophilic fluorescent probe to convey membrane fluidity and polarity information through generalised polarisation values which can be taken at temperature intervals.[67] Similarities in membrane properties between discoidal polymer nanodiscs and bulk bilayers in liposomes, support the claim that polymer lipid particles maintain a lipid bilayer environment analogous to the native cell. Slight differences in lipid properties can also play an imperative role in signalling the occurrence of a transition of lipids from vesicles into nanodiscs.

A marked distinction between lipid bilayers in large unilamellar liposomes (LUVs) and nanoscale lipid discs can be achieved with ^{31}P NMR measurements, wherein the emergence of an isotropic peak, with an area proportional to nanodisc concentration, occurs at the onset of nanodisc formation. This spectral peak is broadened beyond detection for liposome participant phospholipids.[45] Phase diagrams which showcase polymer: lipid molar ratios at the phase boundaries of liposome saturation with polymer ($R_S^{b,SAT} = c_S^{b,SAT}/c_L$) and the eventual complete solubilisation into nanodiscs ($R_S^{m,SOL} = c_S^{m,SOL}/c_L$) can be derived from a series of ^{31}P NMR measurements at different polymer: lipid concentrations. For SMA (3:1, $M_n = 4$ kg mol^{-1}), molar ratios for saturation and solubilisation of 1-palmitoyl-2-oleoyl-*sn*-glycero-3-phosphocholine (POPC) lipid were $R_S^{b,SAT} = 0.099 \pm 0.004$ and $R_L^{m,SOL} = 0.147 \pm 0.005$, respectively.[40] These ratios allow for the calculation of the bilayer to micelle partition

© 2021 Wiley-VCH GmbH

coefficients in addition to corresponding standard values of bilayer-to-micelle transfer free energy ($\triangle G^{\circ}$). Comparable data can be gathered from DLS and more recently, MDS in their ability to deduce R^{SAT} and R^{SOL} parameters. Both of these particle size probing techniques calculate the hydrodynamic diameter (d_H) of particles based on their diffusion coefficient (D) with DLS using a correlation function drawn from the fluctuation of scattered light intensity and MDS using diffusion of the sample under laminar flow with tuneable limits on the size range of particles permitted to migrate between adjacent microfluidic channels.[77,79] The MDS chip set-up employs channels in which the sample and water are run alongside each other before channels split and the diffusion of particles between channels is quantified with primary amine functional labelling (using POPC/POPE 9:1; POPE: 1-palmitoyl-2-oleoyl-*sn*-glycero-3-phosphoethanolamine lipid mixtures for instance). R^{SAT} and R^{SOL} values for POPC/POPE (9:1) LUVs treated with SMA (3:1, $M_n = 4\ kg\,mol^{-1}$) determined by MDS, were 0.07 and 1.03, respectively.[77] Although the R^{SAT} calculation was similar with that determined using ^{31}P NMR, the R^{SOL} value was found to be a large overestimate using MDS compared with other data sources. The presence of POPE in lipid bilayers introduces intrinsic negative curvature which has been found to result in the need for more polymer for its complete nanodisc solubilisation. Moreover,the measured diffusion ratios used to extrapolate R^{SOL} did not account for the shrinkage of nanodisc size (from 30 to 10 nm) at higher polymer: lipid ratios. An amended MDS protocol using hydrodynamic diameter measurements as well as diffusion ratio plots found $R^{SOL\,30\,nm} = 0.36$ which is a more accurate estimate made by specifying 30 nm particles.[77] The high sample polydispersity typical of liposome and nanodisc mixtures is an impediment for accurate determinations of R values using DLS, therefore ^{31}P NMR is the most simple and unambiguous method for constructing phase diagrams representing nanodisc formation. The ability to verify nanoparticle size is, nonetheless, important in verifying the conversion from LUVs into nanodiscs as is shown in the DLS size distributions presented in Figure 4.[28]

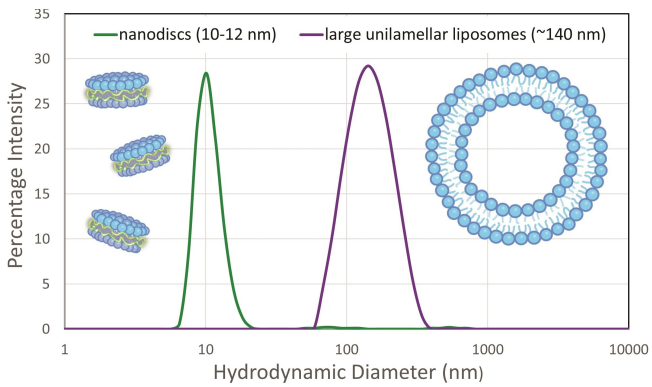

Figure 4. Expected particle size distributions from DLS measurements of both LUV vesicles (blue) and nanodiscs (green) formed upon incubating vesicles with excess SMA accompanied by nanodisc and liposome illustrations.

Particle size as well as detail of particle dimensions and overall nanodisc shape are often best elucidated by SAXS, SANS and specimen tilting cryo-EM approaches. Whereas with particle-size detection methods, analytical ultracentrifugation, SEC and electrophoresis, the dual function of nanodisc purification can also be reliably executed. Analytical ultracentrifugation subjects a sample to a high centrifugal force along with real-time monitoring of particle sedimentation, a process which depends on the diffusion coefficient of the studied material. A simple separation between undissolved liposomes or native membrane fragments and nanodiscs can alternatively be performed using ultracentrifugation (100 000 *g* for 20 h at 4 °C) to gain a sample of soluble nanodiscs within the supernatant.[50] SEC otherwise known a gel filtration, entails the elution of sample through a gel matrix on the basis of size. Columns can be connected to UV–visible, IR, or light scattering detectors to generate a chromatogram indicating the elution volume of free-polymer, liposomes or membrane fragments and nanodiscs.[43] A hydrodynamic radius can be provided by SEC in conjunction with providing monodisperse nanodisc samples. Benefits of preliminary nanodisc purification include a higher accuracy of size and shape measurements with techniques suited to monodisperse samples such as DLS, SAXS and SANS and furthermore, is a prerequisite for most MP characterisation.

4. In Silico Mechanistic Insights

The mechanism of SMA polymer nanodisc formation has long eluded a comprehensive understanding. Recent studies into the parameters which most effectively induce SMALP formation[55] in conjunction with in silico trajectory investigations,[80–81] have shed light in this area. Nile red fluorescence experiments have suggested that membrane solubilisation is able to proceed most effectively when buffer conditions permit a collapsed polymer conformation containing hydrophobic domains as opposed to the random coil conformation.[55] A fine balance which entails a sufficient polymer charge density and hydrophobic polystyrene fractions within SMA sequences was shown necessary for SMALP applications. Computational modelling using the coarse-grained (CG) Martini model has allowed for explorations into the evolution of self-assembled molecular structures of up to microsecond timescales by merging certain individual atoms into pseudo-atoms. Simulations reported by Xue and co-workers[80] using 2:1 SMA copolymers with a periodic monomer sequence, wherein repeated units consisted of 2 Sty and 1 MA with both carboxylate groups deprotonated, demonstrated the concerted behaviour of polymers which adsorbed to the surface of a DDPC planar lipid bilayer. Surface adsorption led to the subsequent perforation and development of polymer stabilised pores in the lipid bilayer. The system ultimately reached a metastable state by the end of the trajectory, wherein polymers were trapped within a largely destroyed lipid bilayer plane. Such an effect was theorised to be an artifact of the periodic boundary conditions chosen for the simulation. Further simulations conducted between the same

© 2021 Wiley-VCH GmbH

SMA copolymers with lipids randomly distributed in the boundary condition box, did self-assemble with one polymer per nanodisc for DDPC and two polymers per nanodisc for longer-chain DPPC. A more representative polymer sample would have involved SMA copolymers with singly deprotonated MA monomers that either showed a statistical (random) or alternating monomer sequence to respectively model coSMA and altSMA versions discussed earlier in this review. A subsequent computational study in a Martini CG force field performed by Orekhov et al., compared 3:1 and 2:1 SMA using singly deprotonated MA, with both periodic and statistical monomer sequences tested for 3:1 SMA.[81] It was found that polymers self-aggregated into clusters in solution and interpolymer cooperation of polymer micelles facilitated polymer insertion into membranes. Although clusters of 2:1 SMA copolymers ultimately resulted in porous membrane end states in simulations, clusters of 3:1 SMA copolymers extracted lipid bundles from the planar bilayer into SMALP-shaped assemblies, maintaining a level of interpolymer association throughout the solubilisation. From this modelled polymer behaviour with reference to prior experimental data, it was proposed that the relative fraction of three subsequent styrene units within polymers was a key determinant in SMALP formation efficiency. Future CG simulations which demonstrate statistical and alternating 2:1 SMA forming SMALPs from a planar bilayer would reinforce this hypothesis.

5. Membrane Protein Research with Polymer Nanodiscs

A variety of membrane protein classes with different properties in terms of size, shape and degree of oligomerisation have been harnessed by SMALPs and other polymer materials by direct solubilisation from native membrane fragments or from synthetic lipid bilayers (most commonly proteoliposomes). Conventional approaches in purifying SMALP-proteins involve affinity chromatography which involve specific binding to the recombinant protein of interest, a popular example of which is the Ni-NTA immobilised metal affinity chromatography strategy that entails engineering the expression of proteins with terminal His-tags in their sequence.[50] In this section, different analytical methods for studying MPs as well as novel purification avenues will be discussed interweaving case studies which reflect the analytical scope offered by polymer nanodisc technology.

5.1. Capture and isolation of oligomeric protein states

Applications of MSP nanodiscs have produced the principle that adjustment of nanodisc diameter to support a critical bilayer area, leads to the ability to selectively harness specific protein oligomers.[27] Most polymer nanodiscs discussed so far can theoretically accommodate a range of diameters depending on their stoichiometry and moreover, possess some flexibility in moulding to the size of a target MP.[49] SMALPs, despite limitations over control of their disc diameter, have been used to capture complexes up to the size of alternative complex III (ACIII) associated in a supercomplex with aa3-type cytochrome c oxidase (ACIII-cyt aa3), with roles in respiratory and photosynthetic electron transport in bacteria. The supercomplex extracted encompasses 48 transmembrane α-helices and has a 464 kDa mass. The extent to which the thin layer of lipid density surrounding SMALP-ACII-cyt aa3 resembled a true bilayer was unclear, although, the coextraction of native lipids was confirmed in cryo-EM analysis and an enhanced stability compared with detergent supercomplex extraction suggested the importance of interacting lipids.[82] The tetrameric potassium channel KcsA was isolated directly from *E. coli* membranes into SMALPs and which was shown to dissociate into its monomeric form upon heat exposure for both detergent and SMA protein extracts. Importantly, the thermostability and durability of the tetramer within SMALP particles was greater than that inside detergent micelles. A close analysis of coextracted lipid by using thin-layer chromatography and quantitative analysis of band intensity, indicated the enrichment of anionic lipids surrounding the KcsA channel in a higher proportion than was found in the total cell lysate. It can be speculated that these specific anionic lipid- protein interactions contribute to sustaining the oligomeric protein structure.[83]

The degree of oligomerisation of proteins and protein complexes within nanodiscs can be measured using techniques such as cryo-EM, negative staining EM, CD[83] as well as sized-based methods like SEC and polyacrylamide gel electrophoresis (PAGE), with the latter offering superior resolution.[78] The compatibility of membrane protein SMALPs with native gel electrophoresis, in which samples travel through a polymer gel matrix with a speed related to their mass to charge ratio under an applied electric current, has recently proved able to conserve the quaternary structure of SMALP embedded proteins throughout gel migration of discrete nanodiscs. The negative charge density and narrow diameter distribution of SMALPs allows membrane proteins, regardless of charge, to migrate through the gel to an extent which reflects the mass of MPs. Accompanied by protein staining techniques such as Coomassie staining and western blotting, SMA has been shown to enable the purification of MPs of a desired degree of oligomerisation without the need to crosslink proteins in situ or engineer proteins. Homodimeric ABC transporter Sav1866 as well as homotrimeric bacterial drug transporter AcrB were excised from their gel band after SMA-PAGE and were directly examined as homogenous samples with cryo-EM. Analytical ultracentrifugation can achieve similar ends in purifying and selecting the oligomeric state of MPs, with SMA-PAGE suited to managing smaller scale samples.

5.2. MP structural characterisation and mechanistic investigations

Cryo-EM, an electron microscopy in which the sample visualised is cooled to cryogenic temperatures, has rapidly gained traction

© 2021 Wiley-VCH GmbH

as an invaluable platform for solving the high-resolution structures of membrane proteins. The allowance for low protein quantities is helpful in MP analysis as there are challenges in recombinantly expressing and purifying large masses of homogeneous MP samples.[52] Before Imaging reconstituted MPs, it is important to confirm that their function within the nanodisc cassette sufficiently imitates their function within their native cellular membrane. SMALPs were once again the membrane mimetic of choice for directly purifying eukaryotic ABC transporter Pgp into native nanodiscs. A fluorescence quenching functional ligand binding assay confirmed the functional activity of Pgp-SMALPs and circular dichroism denoted a predominantly α-helical structure. In tandem with analytical ultracentrifugation, statistical cryo-EM analysis which generated refined low-resolution 3D Pgp structures (Figure 5.), revealed the monomeric nature of the majority of captured Pgp particles.[50]

The overall jellyfish resembling shape, secondary structures and side-chain positions of homotrimeric drug efflux pump, bacterial AcrB, were resolved using cryo-EM at the at resolution 3.2 Å. The presence of 24 hexagonally packed native lipid molecules in the centre of the trimer were able to be detected with cryo-EM imaging, a promising feat in the study of lipid–protein interactions made possible by the detergent-free extraction process of SMA. Such cryo-EM findings unveil insights into the transport mechanism of AcrB. Each protomer of the pump is known to move through three conformational states in coordination with other protomers which exhibit complementary states at any one time. As these transformations occur for a certain protomer, the centrally packed lipid bilayer is positioned to sense, shift position and transduce conformational changes to neighbouring protomers, participating in the coordinated motion of the exporter channel.[52,84]

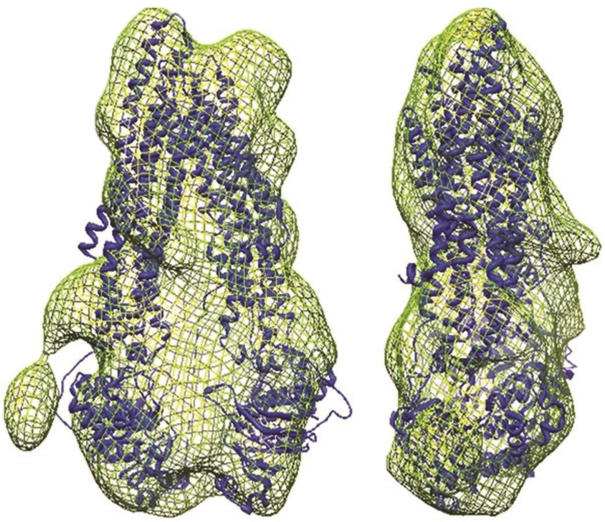

Figure 5. The refined 3D structural envelope of Pgp (green) at ca. 3.5 nm resolution obtained by statistical cryo-EM. The ABCB1 crystal structure (PDB ID: 3G5 U) is superimposed onto the envelope (blue ribbon).[50] This image was reproduced with permission from ref. [50]. Copyright: 2014, Biochemical Society, Portland Press Ltd.

Cyro-EM along with MSP nanodisc cassettes have been employed for investigating the poorly understood molecular mechanism of mammalian ryanodine receptors (RyRs), a homotetrameric channel instrumental in the regulation of muscle contraction. RyR structural architecture was resolved in the closed sate at 6.1 Å and in its open state at 8.5 Å. Isolation of the open state of RyR was promoted by receptor exposure to a buffer concentration of 10 mM Ca^{2+}, as muscle contraction is prompted by Ca^{2+} release from the sarcoplasmic reticulum into the cytoplasm of myocyte cells through RyRs which are activated by the Ca^{2+} influx resulting from an action potential. Comparison of open and closed structures stabilised by lipid nanodiscs led to the mechanistic conclusion that calcium binding to the EF hand domain induces allosterically transmitted conformational changes which ultimately increase the average gate diameter, thus behaving like a Ca^{2+} sensitive switch.[31] Although the last study employed MSP based nanodiscs, it nonetheless showcases the potential for mechanistic investigations of first- or second-generation nanodisc-bound MPs from the provision of high-resolution protein conformer structures.

GPCRs constitute the largest class of MPs in the human genome. Like many receptors, they exist in a dynamic equilibrium between active (R*) and inactive conformations (R) where agonists stabilise R* and antagonists stabilise R. Previous difficulties in isolating GPCRs using conventional detergent purification have resulted from a loss of structural and functional integrity by removing annular lipid which can serve as allosteric regulators of conformational states.[85] SMALPs solubilising the adenosine A_{2a} receptor ($A_{2a}R$) demonstrated a comparable extraction efficiency with detergent micelles with an enhanced thermostability as well as showing undiminished radioligand binding capacity over five freeze-thaw cycles. Changes in the ligand-binding ability of A2aR-SMALPs were related to the unravelling of secondary structure at higher temperatures through CD characterisation, a spectroscopy technique attuned to detect the folding and secondary structure signature of MPs owing to distinctive absorptions of right and left circularly polarised light.[86] CD was also the method used to examine the first reported MP-SMALPs, bacteriorhodopsin (bR) monomers comprised of seven transmembrane helices and eight-stranded β-barrel PagP. Superior thermostability of functional PagP-SMALPs compared with detergent solubilised PagP was likewise confirmed with temperature dependent CD characterisation.[46]

The applicability of SAXS and neutron reflectivity has been demonstrated for resolving the structure and topology of structurally homogenous preparations of integral membrane proteins captured by MSP.[26] Cyt P450 3A4, the drug metabolising enzyme, was embedded into MSP nanodiscs and SAXS was used to localise and determine the shape and orientation of proteins within nanodiscs.[87] The proven ability to adsorb MSP nanodiscs onto analytical surfaces has facilitated similar protein topology investigations using atomic force microscopy,[25] neutron reflectivity and quartz crystal microbalance with dissipation monitoring.[88] Bacteriorhodopsin proton pump reconstituted nanodiscs were adsorbed onto mica and mechan-

© 2021 Wiley-VCH GmbH

ical unfolding by the AFM tip was used to determine intramolecular interactions and protein folding.[89] Depositing an MSP nanodisc film onto a hydrophilic SiO_2 solid support paved the way towards using neutron reflectivity (NR) to observe redox dependent shifts in the conformational equilibrium of cytochrome P450 oxido-reductase (CPR) enzyme catalysing the electron transfer from nicotinamide adenine dinucleotide phosphate (NADPH) to cytochrome P450s. A collection of measurements including neutron reflectivity to model the shape and orientation of CPR conformers, quartz crystal microbalance used to initially confirm the mass deposition and dissipation of the CPR-nanodisc film, and single molecule fluorescenceto assure the identification of CPR enzymes within the nanodiscs - comprising the film. In the absence of NADPH the majority of CPR was in an extended conformation whereas after NADPH addition, the reducing conditions favoured the compact CPR conformer according to NR results. It was posited that the compact version was favoured to protect the reduced FMN cofactor from partaking in unspecific electron transfer.[88] Recently, the ability to absorb a film of empty SMALPs (both coSMALPS and altSMALPS) and SMILPs onto a solid-supported planar lipid bilayer has been shown by neutron reflectivity,[6] therefore each method discussed requiring surface adsorbed nanodisc films could be plausibly adapted to polymer nanodisc studies.

Advanced NMR is a growing arena for MP-nanodisc research with a remarkable ability to provide high resolution protein structures. Examples of advanced NMR approaches include magic angle spinning solid state NMR with subsequent high-resolution 2D NMR signal acquisition for large MP-nanodisc structures and solution 2D NMR used to solve the structures of membrane proteins ranging from small to medium sized.[26] Analogous to bicelles, the size of polymer nanodiscs play a role in whether solution NMR for isotropic nanodiscs or solid-state NMR for larger "macrodiscs" (>20 nm) which can align in an external magnetic field can be employed for analysis.[90] Wagner and colleagues reported the first complete atomic-resolution structural characterisation of an MP (OmpX) within the lipid bilayer environment of an MSP nanodisc showing, with solution NMR, marked differences between OmpX within detergent micelles and encompassed by phospholipid bilayer.[91] By using ^{19}F NMR, transmembrane and soluble domain tryptophan residues of electron donating enzyme cyt b5 were ^{19}F-labeled and reconstituted within 18-residue helical amphipathic (4F) peptidiscs. The ^{19}F NMR spectra facilitated the measurement of ^{19}F–^{19}F distance constraints and effects of phospholipid charge on protein structural integrity. Structures of cyt b5 surrounded in a ring of zwitterionic phospholipids (DMPC specifically), stabilised the expected ^{19}F NMR chemical shifts for cyt b5 transmembrane tryptophans whereas increasing concentrations of anionic lipid POPS, resulted in a significant chemical shift of tryptophan peak positions.[36] Peptide-based nanodiscs have also been used to characterise the structure and dynamics of protein–protein complexes by means of high-resolution NMR spectroscopy shedding light on the interactions of membrane bound cyt P450 2B4, a key metabolic enzyme in liver microsomes, and its electron donor CPR. This was achieved by forming a minimal functional redox complex between the P450 and full-length membrane anchored flavin mononucleotide binding domain (fl-FBD), the redox-active domain of CPR, within 4F nanodiscs.[92–93] In conducting ^{1}H,^{15}N TROSY HSQC analysis, the binding interface of the functional cyt P450-FBD complex was structurally resolved and supported the theory that evolutionarily conserved cyt P450 residue, R125, is involved in the electron transfer from competitive redox partners.[93] The ability of PMA polymer nanodiscs to trap amyloid-beta (Aβ) kinetic intermediate structures which are instrumental in the progression of Alzheimer's disease through the mechanism of membrane assisted aggregation of Aβ peptides, was partly validated using CD and NMR approaches to assign the conformation of $A\beta_{1-40}$ intermediates.[94] Remarkably, the low-order $A\beta_{1-40}$ oligomer trapped by PMA showed reduced neurotoxicity compared with $A\beta_{1-40}$ oligomers in absence of nanodiscs suggesting the therapeutic potential of these findings.

EPR is another technique that is capable of characterising the dynamic properties of MPs residing in SMALP based nanodiscs. Potential for MP-SMALP EPR driven analysis was demonstrated by the study of spin-labelled KCNE1, performed with pulsed EPR titration experiments for phase memory time measurements in addition to CW-EPR titration experiments for EPR spectral line-shape analysis. Experimental results were in agreement with the solution NMR structure of KCNE1 presenting an EPR spectral line broadening which indicated a decreased motion of MP spin labels thought to have been induced by the SMA belt reducing the motion of lipid acyl chains.[95]

Polymer nanodiscs can be valuable tools in the study of MP kinetic intermediates by either artificially stabilising intermediate structures or use of rapid transient characterisation techniques such as rapid mixing spectroscopies and flash photolysis. Polymethacrylate copolymer, as mentioned earlier, was shown to stabilise and provide CD and ThT fluorescence snapshots of a helical intermediate in the aggregation of human islet amyloid polypeptide, which if left to aggregate to its full extent within lipid vesicles, forms a beta sheet structure.[70] Enlisting an MSP lipid nanodisc bracelet for bacteriorhodopsin reconstitution, steady-state and time-resolved spectroscopies comprised of transient absorption and flash photolysis revealed that the photocycle and vibrational dynamics underlying the mechanism of proton pump bacteriorhodopsin, did not deviate between the nanodisc microenvironment and native purple membranes.[96] The advantage of using MSP lipid nanoparticles was an improved signal to noise ratio compared with liposomes and native membranes which allows ground and excited states in the BR photocycle to be clearly assigned, a benefit which could reasonably be generalised to versions of polymer nanodiscs with a high optical transparency.

Research into lipid–protein interactions performed using polymer nanodiscs have so far been discussed in relation to several analytical techniques including cryo-EM, TLC and solution ^{19}F NMR. Native mass spectrometry offers an alternate route to identifying and quantifying annular lipids which support MP structure. Not only can lipids be extracted from a purified MP-nanodisc sample and evaluated in terms of their

© 2021 Wiley-VCH GmbH

overall composition using liquid chromatography mass spectroscopy (LC–MS),[78] but a protocol involving electrospray ionisation – of solubilised nanoparticles followed by gas-phase dissociation allows for the removal of solubilisation agents to study insoluble protein-lipid complexes. This approach has demonstrated capabilities for distinguishing the make-up of surrounding phospholipids in successive lipid layers enrobing MSP reconstituted proteins as increasing gas-phase collision energies causes progressive removal of nanodisc components. The high collision energies required to eject the membrane protein complexes from MSP nanodisc complexes compared with detergent micelles has led to a wider range of MS discernible fragments encompassing intact protein oligomers such as trimeric diacylglycerol kinase (DgkA) enzyme and lipids associated ionically with the structural annular lipid belt that immediately enrobes the MP.[13] Polymer nanodiscs also show promise for adopting similar native mass spectrometry approaches to explore structural and weakly interacting lipids with an MP of interest.

Through employing laser induced liquid bead ion desorption-MS (LILBID-MS), a mid-IR laser was used to dissociate intact and minimally charged MP containing SMALP complexes from small ~50 nm aqueous droplets, thereby producing broad m/z peaks with maximum intensities correlating with average nanodisc mass. Membrane proteins could further be released from their surrounding SMALP construct by a nanosecond laser pulse, a process requiring a threshold energy that brakes up oligomers into constituent monomers.[97] This approach was able to be applied for determining the mass and number of phospholipids encasing monomeric rhomboid protease GlpG, dimeric subunit of the KtrAB high affinity potassium channel KtrB and trimeric multidrug efflux pump AcrB extracted from native *E. coli* membranes. Additionally, the previously unknown oligomerisation states of sodium-solute symporter protein (SSS) and a potassium importer (KimA) were deduced as being monomeric and dimeric respectively by fitting possible oligomeric states to an established linear correlation between the total number of transmembrane helices and additional mass conferred by phospholipids to the nanodisc structure. An alternative native-MS strategy used to reveal specific MP interactions with annular lipids within SMALPs was demonstrated by the extraction of bacteriorhodopsin (bR) and archaerhodopsin-3 (AR3) followed by a nano-electrospray ionisation (nESI) and gas-phase collision protocol ejecting the bR and bound lipids from the nanodisc.[98] This gave high resolution spectra of the fully mature bR protein (after post translational modifications), which was selectively extracted by SMA, bound to exogenous DMPC lipid used in the bR extraction process and endogenous ether-linked lipid 2DP. Native MS studies using SMALPs are an especially recent development which so far can shed light on specific structural lipid–MP interactions, MP oligomerisation and nanodisc composition.

5.3. Ligand-binding functional studies with membrane proteins

A reliable way to test MP function, particularly receptor function, is to test whether they bind their associated ligands in a way which mirrors protein–ligand interactions within native cellular membranes. SMA was used in the first direct detergent-free extraction of a human wild-type GPCR from its native cellular membrane. Dopamine receptors (DRs) prevalent in the central nervous system were solubilised into native SMALPs despite low levels of expression in mammalian cells. Their retention of ligand binding activity was confirmed with radioligand binding assays and microscale thermophoresis which quantifies biomolecular interactions according to the size and charge dependant movement of species in a temperature gradient. This work included the first report of the affinity constant for the association of D1 (wild-type dopamine) receptors with the peptide neurotransmitter neurotensin (NT) in a native lipid environment.[99]

With surface tethered nanodiscs acting as membrane mimetics, more information has been gleaned on changes induced by ligand binding on MP conformational structures and interestingly, the dynamic equilibrium between MP conformers using single molecule and ensemble spectroscopies. Ligand binding on the extracellular region of a GPCR transfers a conformational change to the cytoplasmic surface, this change is recognised by G proteins and a cascade of signalling events are initiated depending on the GPCR and binding ligand. Conformational changes induced for individual receptors by ligand binding were visualised for dye labelled and MSP nanodisc bound β2-adrenergic receptor (β2 AR), a model GPCR, by SMF in the apo form (without ligands) as well as in the presence of pharmaceutical agonists and reverse agonists.[100] MSP nanodiscs were anchored to a streptavidin-coated quartz slide through binding to a biotinylated MSP belt. In all SMF studies, receptors showed basal activity - meaning they were in a dynamic state of fluctuating between active and inactive conformations with inactive conformers exhibiting a distinctive higher fluorescence intensity as displayed in Figure 6. Simultaneous monitoring of individual protein fluorescence trajectories under different ligand exposure conditions showed that rate constants for transitions from inactive to active receptor states were higher in the presence of agonist while in the presence of reverse agonist, the rate constant for shifts to the active state were lowered. Constructed histograms indicating the probability distribution of receptors in active and inactive states after the addition of agonist, showed an equilibrium shift towards the active state of β2 AR and reverse agonists expectantly shifted β2 AR towards a greater occurrence of the inactive conformer.[100]

Similarly, single-molecule total internal fluorescence microscopy was used to demonstrate that the effector ligand, (*R*)-naphthoflavone (ANF), is able to modulate substrate off-rates and thus similarly modulate the dissociation constant (K_D) for Nile Red dye binding to surface tethered MSP captured cyt P450 3A4. In this case nanodiscs were surface tethered with biotinylated lipids. After fitting dwell-time histograms to

© 2021 Wiley-VCH GmbH

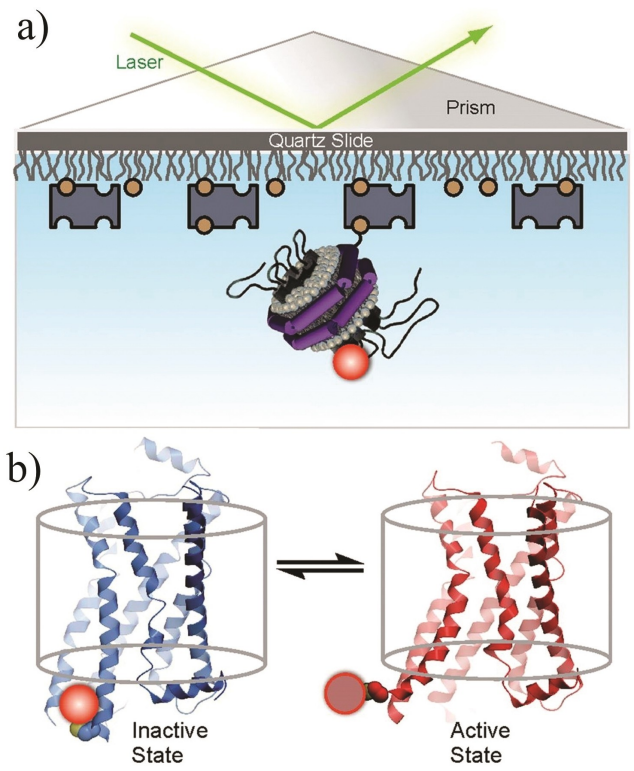

Figure 6. a) A β2 AR receptor protein (black) labelled with Cy3 (red circle) dye within a MSP lipid nanodisc (MSP in purple, phospholipid bilayer in grey) which is surface tethered to a poly(ethylene glycol)-coated quartz slide by the binding of biotin (orange circles) on the MSP belt to streptavidin (dark blue rectangles). The dye-labelled receptor is illuminated with a 532-nm laser beam (green).[100–101] The nanodisc cartoon was adapted courtesy of ref. [100] with permission from ref. [101]. Copyright: 2006, Biotechniques, Future Science Ltd. b) The visual representation of β2 AR receptors transforming between inactive (blue) and active (red) conformers in a lipid bilayer, with associated changes in the local environment of the Cy3 probe resulting in a brighter and dimmer respective fluorescence intensities.[100] Reproduced with permission from ref. [100]. Copyright: 2015, National Academy of Sciences.

exponential decay functions to give K_D values, the substrate off-rate reflecting Nile Red dissociation from cyt P4503A4, was measured $1.5 \pm 0.09\ s^{-1}$. Whereas the effector ANF slowed Nile Red dissociation by 5 times yielding the substrate off-rate of $0.32 \pm 0.05\ s^{-1}$.[102] As has previously been noted, the ability to tether polymer nanodisc belts to a surface has not been yet reported. However, the range of functional groups possible for SMADs, particularly sulfhydryl groups on SMA-SH as well as RAFT end groups for altSMA show potential to be conjugated to surface linkers like biotin and may be applied to analogous SMF studies in the future.

Electrochemical studies on MPs including redox potentiometry and cyclic voltammetry (CV) have been carried out with MSP nanodisc membrane cassettes. Hepatic cyt P450 3A4 is a haem containing redox enzyme active in the metabolism of approximately 50% of drug molecules in humans. With redox potentiometry, a correlation was demonstrated between type I substrate binding to cyt P450 3A4, which are known to induce a shift in the ferric spin state equilibrium to a high spin state, and the redox potential of cyt P450 3A4. Substrate binding was more likely to result in a reduction of the substrate due to the increase in the redox potential of cyt P450 3A4 upon binding substrates. The use of nanodiscs was helpful in stabilising the monomeric cyt P450 3A4 enzyme allowing for unconfounded redox potential measurements.[103] Plant P450s responsible for the biosynthesis of popular commercial compounds (involved in the dhurrin pathway), were individually reconstituted into MSP nanodiscs and immobilised onto gold electrodes. Interest in circumventing the need for NADPH as a biological electron donor by using direct electron transfer from electrodes motivated CV along with TLC analysis of product formation with and without NADPH and carrier proteins for electrode immobilised MP nanodiscs. Cyclic voltammograms revealed stable reversable redox potentials for individual reconstituted cyt P450 79A1, cyt P450 71E1 and CPR enzymes recorded in the presence of tyrosine, oxime and resazurin substrates respectively. Although complete conversion of substrates into products was achieved for surface immobilised enzymes in the presence of NADPH and carrier proteins, electrons channelled directly from the electrode (in the absence of NADPH) did initiate the P450 catalytic cycle but complete conversion into products was not observed.[104] This inability to use direct electrochemistry to convert substrates to products in this work was speculated to be caused by a lack of control over the relay of electrons and efforts to remedy this problem may lead to the implementation redox nano bioreactors and cost-effective screening of potential drug molecules using MSP and prospective synthetic polymer nanodiscs.

Yet another technique which is predicated on the surface tethering of MP encapsulating nanodiscs, is surface plasmon resonance (SPR).[105] Nanodisc solubilised MPs are conjugated to a monolayer coated sensor chip and protein–ligand interactions are monitored through consequent changes in the incident angle of light absorption due to the coherent oscillation frequency of surface conducting electrons excited in the thin metallic sensor material. These electron oscillations are highly sensitive to the refractive index of their surroundings. UV–visible solution and localised surface plasmon resonance (LSPR) studies of nanodisc bound cyt P450 3A4 interactions with type I drugs (typically substrates for enzyme oxidation) and type II inhibitory drugs were undertaken and were able to sense monomeric MP interactions with drug molecules. The LSPR procedure used Ag nanoparticle surfaces created with by nanosphere lithography, which are highly sensitive to changes in the local environment of the nanoparticles. The adoption of a LSPR technique was warranted by the fact conventional SPR sensing methods, based on bulk changes in refractive index, are not suitable to detect interactions of small drug molecules and large protein analytes. Additionally, a strong signal can be produced in conditions where there is spectral overlap in molecular resonances and the LSPR as is the case for haem-containing proteins like cyt P450 3A4.[106] This method is auspicious for potential large-scale drug screening against chromophore-containing membrane proteins.

© 2021 Wiley-VCH GmbH

5.4. Native nanodiscs

Previous discussions about the scope of proven and plausible analytical applications available to polymer nanodiscs, have often raised examples using first-generation MSP nanodiscs and speculated about their transferable applicability to second-generation polymer nanodiscs. One feature unique to polymer nanodiscs, however, is their sought-after ability to directly isolate and solubilise MPs from their native biological membrane with no intervention from detergent forming "native nanodiscs". The first report of native SMALPs presented the extraction of respiratory complexes from the inner membrane in mitochondria in which the membrane disruption from SMA protein extraction was measured by monitoring the dissipation of the pre-existing proton gradient with a fluorescent potentiometric probe. Most protein complexes characterised in native SMALPs were extracted with the same efficiency as detergent and were shown to retain their enzymatic activities.[107] An ability to examine native lipid and protein interactions is conferred by the direct nanodisc coextraction of endogenous lipids typically identified and quantified with TLC, ^{31}P NMR or MS. The direct extraction of cyt b5 from lysed *E. coli* membranes was performed with SMA-EA and a simple 1D ^{31}P NMR experiment identified phosphatidylethanolamine, phosphatidylglycerol and cardiolipin native lipids coextracted with the protein, these are key lipid components found across the *E. coli* membrane revealing no clear lipid preference by cyt b5.[108] Another potential advancement for native nanodiscs (with use of a suitable polymer) stems from their capacity to directly extract a functional library of MPs representing the proteome of specific membrane organelles, an endeavour previously embarked on for MSP nanodiscs to capture functional proteins from mammalian plasma membranes.[109] For native nanodiscs, However, copurified endogenous lipids and the avoidance of detergents introduce fewer disruptions to the native environment of solubilised proteome libraries. Such libraries possess the potential to quickly characterise dysfunctional MPs from patient tissue samples as a biomedical diagnostic approach.

Developments in live-cell fluorescence microscopy have opened opportunities to image the kinetic process of membrane perforation and MP solubilisation from various organelles of human HeLa cells. Fluorescence leakage trajectories showed that SMA disrupts cells in a stepwise process, with initial perforation of the plasma membranes (with significant time variations in leakage from individual cells) before perforating the endoplasmic reticulum within the cell, whereas complete solubilisation of MARCKS, a peripheral plasma membrane protein, was slower than the solubilisation of MPs from cytosolic organelles. Interestingly, the solubilisation of MARCKS which exhibit a tendency to partition into ordered membrane domains was compared with extraction of integral membrane protein NGL3-GFP. Results showed that NGL3 was extracted 1.5 times faster than MARCKS, thus implying an adverse effect of cholesterol-induced lipid packing on native nanodisc solubilisation.[110] It has been found by Swainsbury and co-workers[49] that the solubilisation efficiency of SMA is strongly influenced by the density of protein packing in membranes as well as the size of the protein target. Photosynthetic membranes with high expression of *Rhodobacter sphaeroides* reaction centre complexes (RC-LH1-X) were extremely resistant to extraction by SMA into native nanodiscs whereas reduced RC-LH1-X expression membranes and high expression membranes diluted with fused phospholipids were more amenable to nanodisc solubilisation. The recalcitrance of ordered membrane domains towards SMA extraction presents a challenge in extracting particular MPs from their native biological membrane. There is, however, potential value in using polymer nanodisc forming agents in isolating ordered domains through the selective separation of fluid membrane domains into soluble nanodiscs.

Native nanodiscs can mediate the reconstitution of MPs into other membrane mimetic systems in a detergent-free manner, enabling a range of analytical techniques with preferences for a certain membrane mimetic system. SMALPs were used to solubilise and purify proton pump microbial rhodopsin and transferred the MP into lipid cubic phase where it was subsequently crystallised under cryogenic conditions and analysed with X-ray crystallography to produce a 2.0-Å structure.[42] SMA polymers have shown an incompatibility with somenative-MS methods due to both inherent polymer properties and the heterogeneity of coSMA and therefore protocols to reconstitute the contents of native nanodiscs into amphipols allow the native-MS examination of both the MP and endogenously associated lipids in more compact homogenous nanoparticles.[17] The reconstitution of MP-SMALPs into liposomes and planar lipid bilayers can also be of benefit. When SMA was employed to directly isolate tetrameric potassium channel (KcsA), purified nanodiscs then reconstituted KcsA into a planar bilayer from *E. coli* membrane extract and showed the retained function of the protein through single-channel conductivity measurements observed in real time as KcsA-SMALPs spontaneously fused to the bilayer.[83]

6. Summary and Outlook

Not only can polymer nanodiscs be used to investigate encapsulated membrane proteins, but SMA derivatives have shown promise as vehicles for therapeutic delivery and diagnostic radio imaging.[111] There might also be value in the use of polymer nanodiscs to solubilise tuneable concentrations of MPs for large-scale biocatalysis, direct electrochemistry and biosensors incorporating MPs.[104] This review has explored the history of membrane mimetic technology and focused in detail on synthetic polymer nanodisc materials along with their range of proven and possible analytical applications for revealing the elusive structures, functional mechanisms, and interactions of reconstituted membrane proteins in addition to the unique benefits of native nanodiscs. Such enhanced understandings of membrane proteins have profound implications for drug discovery.

© 2021 Wiley-VCH GmbH

Acknowledgements

M.D.F. thanks Monash University for the award of her RTP stipend PhD scholarship.

Conflict of Interest

The authors declare no conflict of interests.

Keywords: amphipathic copolymers · membrane mimetics · membrane proteins · nanodiscs · styrene maleic acid lipid particles

[1] H. Yin, A. D. Flynn, *Annu. Rev. Biomed. Eng.* **2016**, *18*, 51–76.
[2] H. H. Shen, T. Lithgow, L. Martin, *Int. J. Mol. Sci.* **2013**, *14*, 1589–1607.
[3] M. J. Parmar, M. Lousa Cde, S. P. Muench, A. Goldman, V. L. Postis, *Biochem. Soc. Trans.* **2016**, *44*, 877–882.
[4] J. M. Dorr, S. Scheidelaar, M. C. Koorengevel, J. J. Dominguez, M. Schafer, C. A. van Walree, J. A. Killian, *Eur. Biophys. J.* **2016**, *45*, 3–21.
[5] C. Peetla, A. Stine, V. Labhasetwa, *Mol. Pharm.* **2009**, *6*, 1264–1276.
[6] S. C. L. Hall, L. A. Clifton, C. Tognoloni, K. A. Morrison, T. J. Knowles, C. J. Kinane, T. R. Dafforn, K. J. Edler, T. Arnold, *J. Colloid Interface Sci.* **2020**, *574*, 272–284.
[7] C. Rossi, J. Chopineau, *Eur. Biophys. J.* **2007**, *36*, 955–965.
[8] P. Drucker, V. Gerke, H. J. Galla, *Biochem. Biophys. Res. Commun.* **2014**, *453*, 143–147.
[9] T. Dewa, R. Sugiura, Y. Suemori, M. Sugimoto, T. Takeuchi, A. Hiro, K. Iida, A. T. Gardiner, R. J. Cogdell, M. Nango, *Langmuir* **2006**, *22*, 5412–5418.
[10] L. Renner, T. Pompe, R. Lemaitre, D. Drechsel, C. Werner, *Soft Matter* **2010**, *6*, 5382–5389.
[11] S. H. Park, S. Berkamp, G. A. Cook, M. K. Chan, H. Viadiu, S. J. Opella, *Biochemistry* **2011**, *50*, 8983–8985.
[12] E. Neher, B. Sakmann, J. H. Steinbach, *Eur. J. Phys.* **1978**, *375*, 219–228.
[13] M. T. Marty, K. K. Hoi, C. V. Robinson, *Acc. Chem. Res.* **2016**, *49*, 2459–2467.
[14] T. Ravula, N. Z. Hardin, A. Ramamoorthy, *Chem. Phys. Lipids* **2019**, *219*, 45–49.
[15] C. Tribet, R. Audebert, J. Popot, *Proc. Natl. Acad. Sci. USA* **1996**, *93*, 15047–15050.
[16] A. Marconnet, B. Michon, C. Le Bon, F. Giusti, C. Tribet, M. Zoonens, *Biomacromolecules* **2020**, *21*, 3459–3467.
[17] S. J. Hesketh, D. P. Klebl, A. J. Higgins, M. Thomsen, I. B. Pickles, F. Sobott, A. Sivaprasadarao, V. L. G. Postis, S. P. Muench, *Biochim. Biophys. Acta Biomembr.* **2020**, *1862*, 183192–183192.
[18] C. R. Sanders, B. J. Hare, K. P. Howard, J. H. Prestegard, *Prog. Nucl. Magn. Reson. Spectrosc.* **1994**, *26*, 421–444.
[19] U. H. Durr, M. Gildenberg, A. Ramamoorthy, *Chem. Rev.* **2012**, *112*, 6054–6074.
[20] K. Yamamoto, U. H. Durr, J. Xu, S. C. Im, L. Waskell, A. Ramamoorthy, *Sci. Rep.* **2013**, *3*, 2538.
[21] K. Yamamoto, P. Pearcy, D. K. Lee, C. Yu, S. C. Im, L. Waskell, A. Ramamoorthy, *Langmuir* **2015**, *31*, 1496–1504.
[22] H. Wang, J. Elferich, E. Gouaux, *Nat. Struct. Mol. Biol.* **2012**, *19*, 212–219.
[23] T. Ravula, N. Z. Hardin, G. M. Di Mauro, A. Ramamoorthy, *Eur. Polym. J.* **2018**, *108*, 597–602.
[24] T. H. Bayburt, Y. V. Grinkova, S. G. Sligar, *Nano Lett.* **2002**, *2*, 853–856.
[25] I. G. Denisov, S. G. Sligar, *Chem. Rev.* **2017**, *117*, 4669–4713.
[26] I. G. Denisov, S. G. Sligar, *Nat. Struct. Mol. Biol.* **2016**, *23*, 481–486.
[27] T. H. Bayburt, Y. V. Grinkova, S. G. Sligar, *Arch. Biochem. Biophys.* **2006**, *450*, 215–222.
[28] S. Scheidelaar, M. C. Koorengevel, J. D. Pardo, J. D. Meeldijk, E. Breukink, J. A. Killian, *Biophys. J.* **2015**, *108*, 279–290.
[29] Z. Zhao, M. Zhang, J. M. Hogle, W. M. Shih, G. Wagner, M. L. Nasr, *J. Am. Chem. Soc.* **2018**, *140*, 10639–10643.
[30] K. M. Padmanabha Das, W. M. Shih, G. Wagner, M. L. Nasr, *Front. Biomed. Biotechnol.* **2020**, *8*, 539.
[31] R. G. Efremov, A. Leitner, R. Aebersold, S. Raunser, *Nature* **2015**, *517*, 39–43.
[32] H. Tao, S. C. Lee, A. Moeller, R. S. Roy, F. Y. Siu, J. Zimmermann, R. C. Stevens, C. S. Potter, B. Carragher, Q. Zhang, *Nat. Methods* **2013**, *10*, 759–762.
[33] H. Kariyazono, R. Nadai, R. Miyajima, Y. Takechi-Haraya, T. Baba, A. Shigenaga, K. Okuhira, A. Otaka, H. Saito, *J. Pept. Sci.* **2016**, *22*, 116–122.
[34] M. L. Carlson, J. W. Young, Z. Zhao, L. Fabre, D. Jun, J. Li, J. Li, H. S. Dhupar, I. Wason, A. T. Mills, J. T. Beatty, J. S. Klassen, I. Rouiller, F. Duong, *eLife* **2018**, *7*, e34085.
[35] T. Ravula, D. Ishikuro, N. Kodera, T. Ando, G. M. Anantharamaiah, A. Ramamoorthy, *Chem. Mater.* **2018**, *30*, 3204–3207.
[36] J. Bai, J. Wang, T. Ravula, S. C. Im, G. M. Anantharamaiah, L. Waskell, A. Ramamoorthy, *Biochim. Biophys. Acta Biomembr.* **2020**, *1862*, 183194.
[37] A. Flayhan, H. D. T. Mertens, Y. Ural-Blimke, M. Martinez Molledo, D. I. Svergun, C. Low, *Structure* **2018**, *26*, 345–355.
[38] D. Li, M. Caffrey, *Proc. Natl. Acad. Sci. USA* **2011**, *108*, 8639–8644.
[39] D. Li, M. Caffrey, *Sci. Rep.* **2014**, *4*, 5806.
[40] V. Cherezov, D. M. Rosenbaum, M. A. Hanson, S. G. F. Rasmussen, F. S. Thian, T. S. Kobilka, H. Choi, P. Kuhn, W. I. Weis, B. K. Kobilka, R. C. Stevens, *Science* **2007**, *318*, 1258–1265.
[41] A. Wiśniewska-Becker, W. I. Gruszecki, in *Drug-Biomembrane Interaction Studies: Biomembrane Models* (Ed: R. Pignatello), Woodhead, Cambridge, **2013**, pp. 47–95.
[42] J. Broecker, B. T. Eger, O. P. Ernst, *Structure* **2017**, *25*, 384–392.
[43] S. C. L. Hall, C. Tognoloni, G. J. Price, B. Klumperman, K. J. Edler, T. R. Dafforn, T. Arnold, *Biomacromolecules* **2018**, *19*, 761–772.
[44] J. J. Dominguez Pardo, J. M. Dorr, A. Iyer, R. C. Cox, S. Scheidelaar, M. C. Koorengevel, V. Subramaniam, J. A. Killian, *Eur. Biophys. J.* **2017**, *46*, 91–101.
[45] C. Vargas, R. C. Arenas, E. Frotscher, S. Keller, *Nanoscale* **2015**, *7*, 20685–20696.
[46] T. J. Knowles, R. Finka, C. Smith, Y. Lin, T. Dafforn, M. Overduin, *J. Am. Chem. Soc.* **2009**, *131*, 7484–7485.
[47] S. R. Tonge, B. J. Tighe, *Adv. Drug Delivery Rev.* **2001**, *53*, 109–122.
[48] A. F. Craig, E. E. Clark, I. D. Sahu, R. Zhang, N. D. Frantz, M. S. Al-Abdul-Wahid, C. Dabney-Smith, D. Konkolewicz, G. A. Lorigan, *Biochim. Biophys. Acta Biomembr.* **2016**, *1858*, 2931–2939.
[49] D. J. K. Swainsbury, S. Scheidelaar, N. Foster, R. van Grondelle, J. A. Killian, M. R. Jones, *Biochim. Biophys. Acta Biomembr.* **2017**, *1859*, 2133–2143.
[50] S. Gulati, M. Jamshad, T. J. Knowles, K. A. Morrison, R. Downing, N. Cant, R. Collins, J. B. Koenderink, R. C. Ford, M. Overduin, I. D. Kerr, T. R. Dafforn, A. J. Rothnie, *Biochem. J.* **2014**, *461*, 269–278.
[51] J. F. Bada Juarez, A. J. Harper, P. J. Judge, S. R. Tonge, A. Watts, *Chem. Phys. Lipids* **2019**, *221*, 167–175.
[52] C. Sun, R. B. Gennis, *Chem. Phys. Lipids* **2019**, *221*, 114–119.
[53] A. A. A. Smith, H. E. Autzen, T. Laursen, V. Wu, M. Yen, A. Hall, S. D. Hansen, Y. Cheng, T. Xu, *Biomacromolecules* **2017**, *18*, 3706–3713.
[54] V. Schmidt, J. N. Sturgis, *Biochim. Biophys. Acta Biomembr.* **2018**, *1860*, 777–783.
[55] S. Scheidelaar, M. C. Koorengevel, C. A. van Walree, J. J. Dominguez, J. M. Dorr, J. A. Killian, *Biophys. J.* **2016**, *111*, 1974–1986.
[56] T. Ravula, N. Z. Hardin, J. Bai, S. C. Im, L. Waskell, A. Ramamoorthy, *Chem. Commun.* **2018**, *54*, 9615–9618.
[57] K. M. Burridge, B. D. Harding, I. D. Sahu, M. M. Kearns, R. B. Stowe, M. T. Dolan, R. E. Edelmann, C. Dabney-Smith, R. C. Page, D. Konkolewicz, G. A. Lorigan, *Biomacromolecules* **2020**, *21*, 1274–1284.
[58] T. Ravula, S. K. Ramadugu, G. Di Mauro, A. Ramamoorthy, *Angew. Chem. Int. Ed.* **2017**, *56*, 11466–11470; *Angew. Chem.* **2017**, *129*, 11624–11628.
[59] N. Z. Hardin, V. Kocman, G. M. Di Mauro, T. Ravula, A. Ramamoorthy, *Angew. Chem. Int. Ed.* **2019**, *58*, 17246–17250; *Angew. Chem.* **2019**, *131*, 17406–17410.
[60] G. M. Di Mauro, N. Z. Hardin, A. Ramamoorthy, *Biochim. Biophys. Acta Biomembr.* **2020**, *1862*, 183332.
[61] M. Esmaili, C. Acevedo-Morantes, H. Wille, M. Overduin, *Biochim. Biophys. Acta Biomembr.* **2020**, *1862*, 183360.
[62] S. Lindhoud, V. Carvalho, J. W. Pronk, M. E. Aubin-Tam, *Biomacromolecules* **2016**, *17*, 1516–1522.
[63] M. C. Fiori, Y. Jiang, G. A. Altenberg, H. Liang, *Sci. Rep.* **2017**, *7*, 7432–7410.
[64] M. C. Fiori, W. Zheng, E. Kamilar, G. Simiyu, G. A. Altenberg, H. Liang, *Sci. Rep.* **2020**, *10*, 9940.
[65] T. Ravula, N. Z. Hardin, S. K. Ramadugu, A. Ramamoorthy, *Langmuir* **2017**, *33*, 10655–10662.

© 2021 Wiley-VCH GmbH

[66] S. C. L. Hall, C. Tognoloni, J. Charlton, E. C. Bragginton, A. J. Rothnie, P. Sridhar, M. Wheatley, T. J. Knowles, T. Arnold, K. J. Edler, T. R. Dafforn, *Nanoscale* **2018**, *10*, 10609–10619.
[67] W. Yu, P. T. So, T. French, E. Gratton, *Biophys. J.* **1996**, *70*, 626–636.
[68] M. Tanaka, A. Hosotani, Y. Tachibana, M. Nakano, K. Iwasaki, T. Kawakami, T. Mukai, *Langmuir* **2015**, *31*, 12719–12726.
[69] A. O. Oluwole, B. Danielczak, A. Meister, J. O. Babalola, C. Vargas, S. Keller, *Angew. Chem. Int. Ed.* **2017**, *56*, 1919–1924.
[70] K. Yasuhara, J. Arakida, T. Ravula, S. K. Ramadugu, B. Sahoo, J. I. Kikuchi, A. Ramamoorthy, *J. Am. Chem. Soc.* **2017**, *139*, 18657–18663.
[71] M. Esmaili, C. J. Brown, R. Shaykhutdinov, C. Acevedo-Morantes, Y. L. Wang, H. Wille, R. D. Gandour, S. R. Turner, M. Overduin, *Nanoscale* **2020**, *12*, 16705–16709.
[72] T. Ravula, A. Ramamoorthy, *Angew. Chem. Int. Ed.* **2021**, *60*, 16885–16888; *Angew. Chem.* **2021**, *133*, 17022–17025.
[73] N. Z. Hardin, T. Ravula, G. D. Mauro, A. Ramamoorthy, *Small* **2019**, *15*, e1804813.
[74] P. Stepien, A. Polit, A. Wisniewska-Becker, *Biochim. Biophys. Acta Biomembr.* **2015**, *1848*, 60–66.
[75] R. Zhang, I. D. Sahu, A. P. Bali, C. Dabney-Smith, G. A. Lorigan, *Chem. Phys. Lipids* **2017**, *203*, 19–23.
[76] S. Inagaki, R. Ghirlando, *Nanotechnol. Rev.* **2017**, *6*, 3–14.
[77] M. Azouz, M. Gonin, S. Fiedler, J. Faherty, M. Decossas, C. Cullin, S. Villette, M. Lafleur, D. A. I. S. Lecomte, A. Ciaccafava, *Biochim. Biophys. Acta Biomembr.* **2020**, *1862*, 183215.
[78] N. L. Pollock, M. Rai, K. S. Simon, S. J. Hesketh, A. C. K. Teo, M. Parmar, P. Sridhar, R. Collins, S. C. Lee, Z. N. Stroud, S. E. Bakker, S. P. Muench, C. H. Barton, G. Hurlbut, D. I. Roper, C. J. I. Smith, T. J. Knowles, C. M. Spickett, J. M. East, V. L. G. Postis, T. R. Dafforn, *Biochim. Biophys. Acta Biomembr.* **2019**, *1861*, 1437–1445.
[79] S. Bhattacharjee, *J. Controlled Release* **2016**, *235*, 337–351.
[80] M. Xue, L. Cheng, I. Faustino, W. Guo, S. J. Marrink, *Biophys. J.* **2018**, *115*, 494–502.
[81] P. S. Orekhov, M. E. Bozdaganyan, N. Voskoboynikova, A. Y. Mulkidjanian, H. J. Steinhoff, K. V. Shaitan, *Langmuir* **2019**, *35*, 3748–3758.
[82] C. Sun, S. Benlekbir, P. Venkatakrishnan, Y. Wang, S. Hong, J. Hosler, E. Tajkhorshid, J. L. Rubinstein, R. B. Gennis, *Nature* **2018**, *557*, 123–126.
[83] J. M. Dorr, M. C. Koorengevel, M. Schafer, A. V. Prokofyev, S. Scheidelaar, E. A. van der Cruijsen, T. R. Dafforn, M. Baldus, J. A. Killian, *Proc. Natl. Acad. Sci. USA* **2014**, *111*, 18607–18612.
[84] W. Qiu, Z. Fu, G. G. Xu, R. A. Grassucci, Y. Zhang, J. Frank, W. A. Hendrickson, Y. Guo, *Proc. Natl. Acad. Sci. USA* **2018**, *115*, 12985–12990.
[85] M. Wheatley, J. Charlton, M. Jamshad, S. J. Routledge, S. Bailey, P. J. LaBorde, M. T. Azam, R. T. Logan, R. M. Bill, T. R. Dafforn, D. R. Poyner, *Biochem. Soc. Trans.* **2016**, *44*, 619–623.
[86] M. Jamshad, J. Charlton, Y. P. Lin, S. J. Routledge, Z. Bawa, T. J. Knowles, M. Overduin, N. Dekker, T. R. Dafforn, R. M. Bill, D. R. Poyner, M. Wheatley, *Biosci. Rep.* **2015**, *35*, e00188.
[87] N. Skar-Gislinge, S. A. Kynde, I. G. Denisov, X. Ye, I. Lenov, S. G. Sligar, L. Arleth, *Acta Crystallogr.* **2015**, *71*, 2412–2421.
[88] M. Wadsater, T. Laursen, A. Singha, N. S. Hatzakis, D. Stamou, R. Barker, K. Mortensen, R. Feidenhans'l, B. L. Moller, M. Cardenas, *J. Biol. Chem.* **2012**, *287*, 34596–34603.
[89] M. Zocher, C. Roos, S. Wegmann, P. D. Bosshart, V. Dötsch, F. Bernhard, D. J. Müller, *ACS Nano* **2012**, *6*, 961–971.
[90] T. Ravula, J. Kim, D. K. Lee, A. Ramamoorthy, *Langmuir* **2020**, *36*, 1258–1265.
[91] F. Hagn, M. Etzkorn, T. Raschle, G. Wagner, *J. Am. Chem. Soc.* **2013**, *135*, 1919–1925.
[92] M. Mahajan, T. Ravula, E. Prade, G. M. Anantharamaiah, A. Ramamoorthy, *Chem. Commun.* **2019**, *55*, 5777–5780.
[93] E. Prade, M. Mahajan, S. C. Im, M. Zhang, K. A. Gentry, G. M. Anantharamaiah, L. Waskell, A. Ramamoorthy, *Angew. Chem. Int. Ed.* **2018**, *57*, 8458–8462; *Angew. Chem.* **2018**, *130*, 8594–8598.
[94] B. R. Sahoo, T. Genjo, M. Bekier, S. J. Cox, A. K. Stoddard, M. Ivanova, K. Yasuhara, C. A. Fierke, Y. Wang, A. Ramamoorthy, *Chem. Commun.* **2018**, *54*, 12883–12886.
[95] I. D. Sahu, R. Zhang, M. M. Dunagan, A. F. Craig, G. A. Lorigan, *J. Phys. Chem. B* **2017**, *121*, 5312–5321.
[96] P. J. Johnson, A. Halpin, T. Morizumi, L. S. Brown, V. I. Prokhorenko, O. P. Ernst, R. J. Dwayne Miller, *Phys. Chem. Chem. Phys.* **2014**, *16*, 21310–21320.
[97] N. Hellwig, O. Peetz, Z. Ahdash, I. Tascon, P. J. Booth, V. Mikusevic, M. Diskowski, A. Politis, Y. Hellmich, I. Hanelt, E. Reading, N. Morgner, *Chem. Commun.* **2018**, *54*, 13702–13705.
[98] K. K. Hoi, J. F. Bada Juarez, P. J. Judge, H. Y. Yen, D. Wu, J. Vinals, G. F. Taylor, A. Watts, C. V. Robinson, *Nano Lett.* **2021**, *21*, 2824–2831.
[99] J. F. Bada Juarez, J. C. Munoz-Garcia, R. Inacio Dos Reis, A. Henry, D. McMillan, M. Kriek, M. Wood, C. Vandenplas, Z. Sands, L. Castro, R. Taylor, A. Watts, *Biochim. Biophys. Acta Biomembr.* **2020**, *1862*, 183152.
[100] R. Lamichhane, J. J. Liu, G. Pljevaljcic, K. L. White, E. van der Schans, V. Katritch, R. C. Stevens, K. Wuthrich, D. P. Millar, *Proc. Natl. Acad. Sci. USA* **2015**, *112*, 14254–14259.
[101] A. J. Leitz, T. H. Bayburt, A. N. Barnakov, B. A. Springer, S. G. Sligar, *BioTechniques* **2006**, *40*, 601–610.
[102] A. Nath, P. K. Koo, E. Rhoades, W. M. Atkins, *J. Am. Chem. Soc.* **2008**, *130*, 15746–15747.
[103] A. Das, Y. V. Grinkova, S. G. Sligar, *J. Am. Chem. Soc.* **2007**, *129*, 13778–13779.
[104] K. Bavishi, T. Laursen, K. L. Martinez, B. L. Moller, E. A. Della Pia, *Sci. Rep.* **2016**, *6*, 29459.
[105] M. Trahey, M. J. Li, H. Kwon, E. L. Woodahl, W. D. McClary, W. M. Atkins, *Curr. Protoc. Protein Sci.* **2015**, *81*, 29.13.21-29.13.16.
[106] A. Das, J. Zhao, G. C. Schatz, S. G. Sligar, R. P. Van Duyne, *Anal. Chem.* **2009**, *81*, 3754–3759.
[107] A. R. Long, C. C. O. Brien, K. Malhotra, C. T. Schwall, A. D. Albert, A. Watts, N. N. Alder, *BMC Biotechnol.* **2013**, *13*, 1–10.
[108] B. Krishnarjuna, T. Ravula, A. Ramamoorthy, *Chem. Commun.* **2020**, *56*, 6511–6514.
[109] J. Roy, H. Pondenis, T. M. Fan, A. Das, *Biochemistry* **2015**, *54*, 6299–6302.
[110] J. M. Dorr, M. H. van Coevorden-Hameete, C. C. Hoogenraad, J. A. Killian, *Biochim. Biophys. Acta Biomembr.* **2017**, *1859*, 2155–2160.
[111] M. Tanaka, A. Hosotani, T. Mukai, *J. Labelled Compd. Radiopharm.* **2018**, *61*, 857–863.

Manuscript received: May 3, 2021
Accepted manuscript online: June 27, 2021
Version of record online: July 30, 2021

© 2021 Wiley-VCH GmbH